

HYPERSPECTRAL REMOTE SENSING OF FIRE INDUCED  
WATER REPELLENT SOILS

By

SARAH ANN LEWIS

A thesis submitted in partial fulfillment of  
the requirements for the degree of  
MASTER OF SCIENCE IN ENGINEERING

WASHINGTON STATE UNIVERSITY  
College of Engineering and Architecture

DECEMBER 2003

To the Faculty of Washington State University:

The members of the Committee appointed to examine the thesis of SARAH ANN LEWIS find it satisfactory and recommend that it be accepted.

---

Chair

---

---

---

---

## ACKNOWLEDGEMENTS

To start, I would like to thank all of my committee members for their knowledge, patience, and support. My research advisor, Joan Wu, provided many hours of help with the data analysis and writing the two journal articles. Joan was always there for a last minute meeting and each time had ready words of encouragement. Special thanks also to Pete Robichaud who provided the idea and the expertise, in addition to a great financial and personal investment. Pete's enthusiasm for this project kept me going through the most frustrating times. Thanks to Bruce Frazier for an introduction to remote sensing and for teaching me how to analyze the data. And finally, thanks to Bill Elliot who kept my project down to earth and has always provided great professional advice.

A huge thank you to the field crews who helped me collect data in Colorado last summer: Pete Robichaud (again), Bob Brown, Troy Hensiek, Jared Yost, and Kevin Spigel from RMRS, Moscow; Karen Jennings and Christine E. from Riverside, CA; Annette Parsons, Michael Parenti and Suzie Loadholt from 2002 Forest Service BAER teams; and Ray Kokaly from the USGS in Denver. I would probably still be doing water drop tests in Colorado if it weren't for your help and for the long hours you all put in. Thank you to Denise Laes (RSAC, Salt Lake City) for your help with the data analysis and for answering a ton of my questions. Thank you to Paul Swetik (RMRS, Moscow) for your technical and computer support as well as your friendship. Thanks also to Andy Hudak, Carter Stone, Don Shipton, Jon Sandquist (RMRS, Moscow) and Penny Morgan (University of Idaho) for collecting more data with me this fall, and for keeping me sane during the crazy last

couple of months of this project. You are all great to work with and to play with; I don't know with who would be better to spend weeks at a time in the field.

Thank you to my IGERT advisors: Jim Petersen, David Yonge, Abby Coleman, Brent Peyton, Markus Flury, Shulin Chen, and to several of my fellow IGERT students: Maya Place, Jennifer Hudson, Jennifer Shaltanis, Irra Sundram, Laura Wendling, Bill Johnson, Brit Johnson, and others. You were all motivating, helpful and fun to work with during the last three years. Thank you to my hydrology research group. You were very supportive and encouraging; in spite of being very busy yourselves. I didn't get to work with Ashley Covert and Lonnie Newton (RMRS and U of I) on this project, but their company in several graduate classes and on previous field trips was very much appreciated.

My friends from Pete's B&G were a great emotional backbone and were always there when I needed to relax and laugh. Holly, Julie, Meghan, Traci, Cory, Nick, Andy, Ed, Eric, and everyone else during the past several years. A special thanks to Bob Scholes and Alyssa Swanson, for being wonderful friends and for having so much confidence in me. Thank you to my parents, to my brother Erik and his family, and to Janel and her family, for all of your love and support. Grad school, and my life, wouldn't have been the same experience without any of you.

HYPERSPECTRAL REMOTE SENSING OF FIRE INDUCED  
WATER REPELLENT SOILS

Abstract

By Sarah Ann Lewis, M.S.  
Washington State University  
December 2003

Chair: Joan Wu

The summer of 2002 was one of the worst fire seasons in history, especially for the state of Colorado where the Hayman Fire burned nearly 60,000 ha. Almost a third of the fire was classified as a high severity burn, which often translates into a high erosion potential. After a fire, soils are frequently rendered water repellent due to the burning of vegetation and surface organic matter. Two methods of testing water repellent soils were performed on the Hayman Fire, the traditional water drop penetration time (WDPT) test and a new mini-disk infiltrometer test. The ability of these two methods to identify water repellent soils in relation to burn severity was tested as well as the compatibility between the tests. The moderately burned sites exhibited the strongest and most persistent water repellency according to both WDPT and infiltrometer tests. The WDPT and infiltrometer values were correlated for each individual burn severity class as well as overall. As the infiltrometer is still in experimental stages, we recommend both tests be used for method comparison and evaluation.

After evaluation of the ground data, a hyperspectral image that was acquired after the fire was analyzed in an attempt to remotely identify soil water repellency. Remote detection of organic matter in soils has been studied extensively and wavebands that were previously identified as useful were analyzed for spectral features indicative of water repellency. No features were found to correlate well with soil water repellency, mostly because of the overall dampening the blackness from the fire had on soil spectral signatures. A supervised classification was run with the mean spectral signatures of low, moderate and high water repellency soils as endmembers. The accuracy of the classification for identifying the degree of severity of soil water repellency was low, but the ability to identify the presence of soil water repellency was nearly 80 percent. According to the classification, approximately 20 percent of the Hayman Fire was at a high risk for soil erosion, and these are the areas on which erosion mitigation should be focused.

## TABLE OF CONTENTS

	Page
ACKNOWLEDGEMENTS.....	iii
ABSTRACT.....	v
LIST OF TABLES.....	viii
LIST OF FIGURES.....	ix
CHAPTER	
1. INTRODUCTION.....	1
2. DETERMINING FIRE INDUCED SOIL WATER REPELLENCY USING WATER DROP PENETRATION TIME AND MINI-DISK INFILTROMETER TESTS.....	6
3. HYPERSPECTRAL REMOTE SENSING OF WATER REPELLENT SOILS AFTER THE HAYMAN FIRE, COLORADO.....	31
4. CONCLUSION.....	71
APPENDIX	
A. FIELD DATA FORMS AND INSTRUCTIONS.....	75
B. WATER REPELLENCY DATA.....	81
C. BURN SEVERITY DATA.....	85
D. EXAMPLES FROM SAS: STATISTICAL CODE AND OUTPUT.....	92
E. SAMPLE EIGENVECTOR AND COVARIANCE STATISTICS FROM PRINCIPAL COMPONENT BANDS 1–10.....	97
F. PICTURES.....	100

## LIST OF TABLES

1. P1 Table 1. Water repellency tests, ground cover, vegetation, and topography variables in order of their significance for determining burn severity.....	26
2. P1 Table 2. Correlation between significant burn severity variables and water repellency test variables.....	28
3. P2 Table 1. ANOVA statistics testing for WDPT correlation with wavebands and Tukey means test comparing means of water repellency classes across waveband ranges.....	61
4. P2 Table 2. Soil characteristics and ground cover characteristics by flight line and water repellency severity classes.....	62
5. P2 Table 3. Classification matrix of FL4 with 50% of the study plots as validation pixels.....	63
6. P2 Table 4. Classification matrix of FL7 with 50% of the study plots as validation pixels.....	64

## LIST OF FIGURES

1. P1 Figure 1. Hayman Fire location in Colorado, sample plot locations within the fire, and the transect layout.....	29
2. P1 Figure 2. Distribution of water repellency measurements at low, moderate, and high burn severities.....	30
3. P2 Figure 1. Hayman Fire location, sample plot locations within fire, transect layout, and locations of FL4 and FL7.....	65
4. P2 Figure 2. Mean reflectance values for the three water repellency endmembers for both flight lines across all measured wavebands.....	66
5. P2 Figure 3. Soil, water, green and black vegetation endmembers plotted across all measured wavebands.....	67
6. P2 Figure 4. Images of FL4. One RGB image, one PC image, one SAM classified image of water repellency classes.....	68
7. P2 Figure 5. Images of FL7. One RGB image, one PC image, one SAM classified image of water repellency classes.....	69
8. P2 Figure 6. Close-up of FL7 image and one plot with adjacent pixels.....	70

## CHAPTER ONE

### INTRODUCTION

Forest fires dramatically effect many aspects of the environments in which they occur. The immediate effects, such as the destruction of vegetation is clearly evident and relatively easy to evaluate. Minor consequences, including the alteration of soil structure and composition and consumption of small fuels, are more complex to quantify. As inconsequential as these micro-transformations may seem, they often have much larger implications for the surrounding areas. As the organic material, such as litter and duff on the soil surface, is consumed in a fire, chemical changes often occur within the upper soil layers. Volatilized organics emit vapors that are distributed in the soil profile (DeBano *et al.*, 1976). As the organic vapors cool, soil particles are coated by a hydrophobic organic layer, consisting primarily of aliphatic hydrocarbons (Savage *et al.*, 1972). The formation of these water repellent soils has a negative effect on the soil's hydrologic condition. The soil's ability to infiltrate water is considerably decreased and the effects of this phenomenon are frequently seen for two years or more following the fire (Pierson *et al.*, 2001; Robichaud, 2000). Decreased infiltration means increased soil erosion potential when high intensity rain falls on the disturbed soil surface (DeBano, 2000b; Robichaud, 2000; Shakesby *et al.*, 2000; Wang *et al.*, 2000). High rates of rainfall runoff and soil erosion lead to roads being washed out, sediment in lakes and streams, and the possible loss of structures that may fall in the path of debris flows. The greatest risk for increased erosion is during high intensity rain events in the first year after the fire. Runoff and soil

erosion levels are frequently one to three orders of magnitude greater than the pre-fire level in the year following a high severity fire (Benavides-Solorio and MacDonald, 2001; Robichaud et al., 2000).

In order to predict areas that are affected by a decreased infiltration rate and sequential increased risk of erosion, soils are tested with one of several tests. These are *in situ* tests that essentially quantify the time a drop of water will remain on the soil's surface without infiltrating. These tests, the water drop penetration time (WDPT) test, the critical surface tension (CST) test, and the mini-disk infiltration test, require several seconds to several minutes per test and must be replicated many times within the area of interest in order to determine the average capability of the soil to infiltrate water (Lewis *et al.*, 2003; Huffman *et al.*, 2001; Letey *et al.*, 2000). The WDPT and CST are well-established tests, whereas the mini-disk infiltrometer has not been extensively tested in the field. The infiltrometer is thought to be less subjective and less time consuming than either of the two traditional tests. The potential for this test to either replace one of the conventional tests or provide additional hydrologic soil information seems promising, and is tested in the first of the following papers. However, caution must be used when using these tests as they are point measurements; thus, making inferences for a large fire challenging.

Remote sensing of environmental conditions and attributes, such as vegetation, soil and the atmosphere are several areas in which this technology is becoming common. Spectral remote sensing is useful for detecting vegetation types, land covers, soil water content, organic matter (OM) content, soil texture and soil mineral content (Chang and Islam, 2000; Jackson and LeVine, 1996; Jackson *et al.*, 1995). Environmental change

analysis and environmental risk assessment are two areas that have recently benefited from remote sensing advances. Remote sensing is a commonly used tool for quick burn severity assessment after large forest fires (Remote Sensing Applications Center, 2003). USDA Forest Service Burned Area Emergency Rehabilitation (BAER) teams and USDI stabilization and restoration teams ground validate a postfire remotely sensed image in the initial days following a fire before recommending rehabilitation treatments. The maps are quickly made from a low-resolution satellite image, such as LANDSAT or SPOT. Rapid as these maps and techniques may be, the accuracy has been questioned, as well as the applicability to diverse ecosystems. With new satellite and imagery technology, remotely sensed images are higher quality and more accessible than ever. Using a very high spatial and spectral resolution instrument, such as hyperspectral, may produce a higher quality image that is more useful than the current burn severity maps. Higher spatial resolution may allow for a more precise prediction of at-risk regions in a fire perimeter and higher spectral resolution provides more wavebands of data that may allow for more advanced image processing techniques and subsequent image classification.

Although remote sensing of water repellent soils has not been attempted specifically, the ability to remotely sense related soil properties, such as soil moisture, soil OM, and soil texture and type, has been very successful (Chang and Islam, 2000; Palacios-Orueta and Ustin, 1998; Jackson and LeVine, 1996; Coleman and Montgomery, 1987). Soil organic properties are spectrally identifiable in the visible range and especially in the near- and short-wave infrared regions of the spectrum (Fidencio *et al.*, 2002; Hummel *et al.*, 2001; Ben-Dor and Banin, 1995; Henderson *et al.*, 1992). The relationship between

soil water repellency and the change in organic properties of the soil as a result of forest fires builds a convincing argument for remote sensing of soil water repellency.

Two independent papers follow, both with the goal of a better assessment of postfire soil conditions, yet with their own specific objectives. All data were collected after the Hayman Fire in Colorado, in the summer of 2002. The title of the first paper is “*Determining fire-induced soil water repellency using water drop penetration time and mini-disk infiltrometer tests*”. The objectives of this paper were: (1) to verify the assigned burn severity classes based on the BAER burn severity map and to identify the most significant soil and vegetation characteristics for *in situ* determination of burn severity and soil water repellency; (2) to determine water repellency of soils in the field using two methods, the WDPT and infiltrometer tests, and to compare their results; and (3) to relate soil water repellency to burn severity classes. The title of the second paper is “*Hyperspectral remote sensing of water repellent soils after the Hayman Fire, Colorado*”. The objectives of this paper were: (1) to determine whether organic properties of the study soils are identifiable spectrally and whether there are differences among low, moderate, and high water repellency soils based on these organic spectral features; (2) to determine which waveband(s) have the strongest correlation with water repellent soils; and (3) to use water repellency ground data to perform a supervised classification on two typical flight lines of hyperspectral data obtained on the Hayman Fire. Conclusions are presented separately in both papers, and there is also a concluding chapter evaluating all objectives and their relevance to postfire erosion.

The authorship of the two following papers is shared between myself and my graduate committee advisors. I am the first author of both papers and wrote the majority of both with the guidance, expertise and suggestions provided by the co-authors. Both papers will be submitted to the journal *Hydrological Processes* and all tables, figures and references are in the journal specified format.

## CHAPTER TWO

### DETERMINING FIRE INDUCED SOIL WATER REPELLENCY USING WATER DROP PENETRATION TIME AND MINI-DISK INFILTROMETER TESTS

Sarah A. Lewis, Joan Q. Wu and Peter R. Robichaud

#### **Abstract**

The summer of 2002 was one of the worst fire seasons in history, especially for the state of Colorado where the Hayman Fire burned nearly 60,000-ha. Almost a third of the fire was classified as a high severity burn, which often translates into a high or very high erosion potential. Soil and vegetation conditions were measured in order to classify burn severity and to validate a remotely sensed soil burn severity map. After a fire, soils are frequently rendered water repellent due to the burning of vegetation and surface organic matter. Fire-induced soil water repellency is often assumed to be related to increasing site burn severity. Two methods of testing water repellent soils were performed on the Hayman Fire, the traditional water drop penetration time (WDPT) test and a new mini-disk infiltrometer test. The ability of these two methods to identify water repellent soils in relation to burn severity was tested as well as the compatibility between the tests. Soil water repellency did not necessarily increase with increasing burn severity. The moderately burned sites exhibited the strongest water repellency according to both WDPT and infiltrometer tests. The WDPT and infiltrometer values were correlated for each individual burn severity class as well as overall. As the infiltrometer is still in experimental stages, we recommend both tests be used for method comparison and evaluation.

## Introduction

Forest fires are the cause of many physical and chemical changes in soil properties, such as particle size, soil water content, pH, organic matter (OM) content and porosity (Nishita and Haug, 1972). Soil moisture decreases during burning, while pH has an overall increase (Nishita and Haug, 1972). Soil OM begins combustion at 210°C, and the content steadily decreases with increasing temperature (Giovannini and Lucchesi, 1997). Soil porosity decreases, partly due to the combustion of OM and subsequent breakdown in structure.

As surface vegetation is burned and the soil is heated, OM in the soil is volatilized and a considerable portion of the gaseous cloud moves from the surface further into the soil (DeBano *et al.*, 1976). As the soil cools, or as cooler soil is encountered, organic hydrophobic substances, comprised primarily of aliphatic hydrocarbons (Savage *et al.*, 1972), coat soil particles and form a water repellent layer. This non-continuous water repellent layer is generally within the top 50 mm of the soil profile, parallel to the surface (Clothier *et al.*, 2000; DeBano, 2000a). The severity of the fire, commonly defined by its intensity, temperature, and duration, affects the degree of soil water repellency, as do the initial soil water and OM contents (DeBano, 2000a). Generally, there is a positive correlation between soil water repellency and the severity of the fire up to a threshold temperature. Temperatures up to 280°C contribute to hydrophobic substances coating soil particles, while temperatures above this point often break down hydrophobic bonds (DeBano, 2000b; Letey, 2001). The loss of soil water repellency most commonly occurs at the soil surface because temperatures are greatest at the surface during a fire, and decrease

with depth. This is why soil is often initially wettable after a fire, yet the water repellent layer still exists and hinders infiltration when the wetting front reaches the non-wettable water repellent layer.

Water repellent soils may affect the hydrologic response of a burned area after a wildfire. The removal of protective vegetative cover and weakening of soil structure leaves the soil unstable and vulnerable to erosion (Robichaud, 2000). These disturbed soils have been identified as a key factor in postfire erosion (Huffman *et al.*, 2001; Pierson *et al.*, 2001; Robichaud, 2000). Decreased infiltration capacity combined with an increase of bare soil often lead to increased runoff, sedimentation, and the formation of rills (DeBano, 2000b; Robichaud, 2000; Shakesby *et al.*, 2000; Wang *et al.*, 2000). Record erosion rates on the order of one to three magnitudes greater result if high-intensity rainfall exceeds the infiltration capacity of the soil shortly after a fire (DeBano, 2000b; Robichaud *et al.*, 2000).

The most widely used technique for testing water repellent soils is the water drop penetration time (WDPT) test (Letey *et al.*, 2000; Wang *et al.*, 2000). In this test, a water drop is placed on the soil surface and if it does not infiltrate in five seconds, the soil is classified as water repellent. Soils that infiltrate the water drop are classified as wettable. WDPT is used extensively due to its simplicity and ability to quickly identify the presence of water repellent soils (Letey *et al.*, 2000). Problems with the WDPT include the subjectivity in the size of the water drop used and the time it takes to identify a highly (five minutes) or a severely (60 minutes) water repellent soil (Dekker and Ritsema, 1994).

A new method, the infiltrometer test, has been recently designed and uses a portable mini-disk infiltrometer (Decagon Devices, Inc., Pullman, WA). In an infiltrometer test, the time to the start of infiltration is measured, as in a WDPT test. In addition, the amount of water that infiltrates into the soil in the first minute of infiltration is measured and taken into consideration when determining the degree of water repellency. Compared to the WDPT method, the infiltrometer test is less subjective, easier to use, and may provide more hydrologic information about the soil.

For large wildfires, postfire condition evaluation is regularly performed by US Federal Agency Burned Area Emergency Rehabilitation (BAER) teams. Developing a postfire soil burn severity map is generally the first step in the evaluation process. The burn severity map is intended to be used for a quick assessment of fire-induced changes to soils and runoff and erosion potential (Parsons, 2003, unpublished report).

In developing the burn severity map, multi-spectral satellite imagery (MODIS) is used to first generate a reflectance map of the burn site. The reflectance spectra are classified using an existing algorithm (Remote Sensing Application Center, 2003) to create a map of increasing soil burn severity. On the ground, low soil burn severity generally has minimal soil heating and slight or no change in soil structure or potential runoff response. In contrast, high soil burn severity typically includes moderate to high soil heating, complete surface organic material combustion, change in soil structure, and a resulting high potential for runoff and erosion (Ryan and Noste, 1983; Parsons, 2003, unpublished report). Upon completion, the burn severity map is validated in the field. Generally the ground truthing by the BAER team is minimal due to time constraints, however on the

Hayman, the extensive data collected for this study will allow for a very thorough validation of the map. Burn severity is classified in the field by evaluating the canopy and ground surface immediately after the fire. Many of the factors are used in the classification are subjective, e.g. soil color (brown, black, red, or white), canopy color (green, brown, or black), and degree of char, as well as the visual estimation of percent ground cover of each factor (Jain, 2002, unpublished study plan). Identifying and standardizing the soil and vegetation characteristics that are most significant for determining burn severity and soil water repellency is thus highly desirable.

A comprehensive USDA Forest Service, Rocky Mountain Research Station project is underway on the Hayman Fire in central Colorado. A major objective of the project is to examine the most modern remote sensing techniques as a potential tool for rapidly, efficiently, and accurately determining burn severity and soil water repellency to expedite the identification of high-risk areas for soil erosion. Another objective was to examine the relationship between soil burn severity and water repellency. The relationship, however imprecise, provides a promising solution to the problem of identification of postfire erosion potential. Remote sensing images from Hayman are currently being processed and the analysis results will be reported in a separate paper. This study focused on relating burn severity and soil water repellency after wildfires. The specific objectives were: (1) to verify the assigned burn severity classes based on the BAER burn severity map and to identify the most significant soil and vegetation characteristics for *in situ* determination of burn severity and soil water repellency; (2) to determine water repellency of soils in the field

using two methods, the WDPT and infiltrometer tests, and to compare their results; and (3) to relate soil water repellency to burn severity classes.

## **Materials and Methods**

### *Study Area*

The study was conducted on the 55,900-ha Hayman Fire located on the Pike and San Isabelle National Forests in central Colorado (Figure 1). The fire started in early June and burned through August of 2002. The Hayman Fire was the largest in Colorado fire history. Thirty-one percent of the total area was classified as low soil burn severity, 20 percent as moderate, 32 percent as high, and 17 percent was unburned (USFS, 2002). The elevation of the fire site ranges from 1,700 m at the base of the fire to about 3,600 m at the highest peaks within the fire perimeter. Slopes are typically 10 to 50 percent. The site receives average annual precipitation of 500 mm. January is the coldest month, with an average temperature of 0°C at the lower elevations and -5°C at the higher elevations. July is the warmest month, with an average temperature range of 18 to 15°C at the lower and higher elevations, respectively (Colorado Climate Center, 2002). The region is semi-arid, with a late summer monsoon season that often delivers short-duration, high-intensity storms.

The dominant canopy vegetation is ponderosa pine (*Pinus ponderosa*) and Douglas fir (*Pseudotsuga menziesii*). Above 2,600 m, vegetation includes sub-alpine forest: lodgepole pine (*Pinus contorta* var. *latifolia*), limber pine (*Pinus flexilis*), aspen (*Populus tremuloides*), subalpine fir (*Abies lasiocarpa*), and Englemann spruce (*Picea engelmannii*)

(Romme *et al.*, 2002) and the soils are mostly granitic. The region is underlain by the Pikes Peak batholith, with frequent rocky outcroppings (USFS, 2002). The two main soil types are Sphinx and Legault, which are both coarse-textured and gravelly and often overly drained (Robichaud *et al.*, 2002). Sandy loams, gravelly sandy loams, and clay loams make up the remaining soils within the fire perimeter (Cipra *et al.*, 2002).

### *Sampling Scheme*

Approximately sixty sample points were selected in each of the three burn severity classes as determined remotely by the BAER soil burn severity map (low, moderate, and high) for a total of 182 sample points. Points were positioned along east-west transects that were ideally 200 m in length (Figure 1). The actual length of transects was between 50 and 400 m (6 to 18 sample points each) as topography would allow. In the low burn severity class there were eight transects with a total of 63 sample points; two transects with six points each and six transects with nine points each. In the moderate burn severity class, there were seven transects for a total of 59 sample points (one sample point was discarded due to bad data). And in the high burn severity class, there were six transects for a total of 60 sample points. Each transect endpoint (locations 0 and 200 m), as well as the point 50 m from the west endpoint, were referred to as central reference points. Extending from each central point were three 20-m radials in the azimuthal directions 0, 120 and 240 degrees, respectively. The actual sample points were located at the end of each of these radials. The spatial and directional layout of the transects and sample points was used to account for the

high spatial variability of environmental data. Each sample point was a 4-m diameter circle in which all burn severity and water repellency measurements were made.

### *Burn Severity Assessment*

At each sample point, the burn severity was assessed by observing and measuring 21 variables indicating soil, vegetation, and topography conditions (Jain, 2002, unpublished study plan). Visually, the degree of burn of soil and remaining vegetation was estimated by color and composition (Ryan and Noste, 1983). Brown soil is generally unburned or lightly burned while black or red soil is severely burned. Vegetation varies from green (unburned) to yellow or brown (moderately burned) to black (severely burned). The percent surface cover for the 4-m circle was visually divided into ten categories. Among these variables were ash and mineral soil percent surface cover, as well as new litter (mainly postfire needle cast) and pre-fire litter percent cover and depth. The percent char (percent black) of small (diameter less than 80 mm) and large (diameter greater than 80 mm) coarse woody debris, stumps, saplings (diameter at breast height [dbh] greater than 25 mm and less than 120 mm), and shrubs were measured. The number of new tree seedlings (dbh less than 25 mm), shrubs and saplings was also tallied. Live and burned trees were counted, measured, and the percent char estimated. An undisturbed soil sample was taken at the mineral soil surface (up to 25 mm depth) within each plot. A digital photograph was taken at each sample point for a visual reference encompassing the 4-m circle. GPS measurements were made at the endpoints of each of the transects as well as at other points on the transects for additional location reference.

### *Water Repellency Tests*

The WDPT test was replicated 11 times along a 0.5-m line transect within each 4-m circle. Surface ash and litter were gently swept aside to reveal the bare mineral soil. At each of the 11 points along the line, a water drop was placed on the soil surface and the time to infiltration was measured. If the water drop remained on the soil surface for longer than five seconds, the soil was considered water repellent (DeBano, 2000b; Letey *et al.*, 2000). The water drop was allowed to remain on the surface for up to 360 seconds to determine the degree of soil water repellency. Water repellency was divided into three classes by the average time to water drop infiltration per plot: low (6 to 60 s), moderate (61 to 180 s), and high (181 to 300 s) (Dekker and Ritsema, 1994).

On a line parallel to and within 200 mm directly above or below the WDPT test line, infiltrometer tests were performed to measure the time to the start of infiltration and the volume of water that infiltrated in one minute. The field-portable mini-disk infiltrometer had a constant pressure head of five mm and measures the volume of cumulative infiltration per time over a known area. The mini-disk infiltrometer was filled with water and placed on the bare soil surface at four evenly spaced locations along the line. In order to minimize lateral flow, care was taken to not let soil or ash touch the sides of the porous plate. The time to the start of infiltration was noted, as was the volume of water that infiltrated into the soil within the first minute of infiltration.

### *Organic Matter Determination*

A laboratory dry combustion procedure (loss on ignition) was performed on all soil samples taken from the 182 sampling points at the study site in order to determine the OM content (Smith and Atkinson, 1975). Soil samples were dried at 105°C for 24 hours to remove moisture. Dry samples were then placed in a muffle furnace set at a temperature of 375°C for 16 hours to incinerate all OM. Upon cooling to room temperature, the percentage of soil OM was calculated by mass.

### *Statistical Analysis*

Normality tests were first performed on the water drop and infiltrometer data with SAS (SAS Institute Inc., 1990). The data were either pooled or sub-grouped by burn severity class. Normality tests were also performed on all other burn severity variables. All tests results indicated non-normal distribution for all samples (see also Fig. 2). Therefore, nonparametric analysis was used for subsequent statistical tests.

A one-way nonparametric analysis of variance with the Kruskal-Wallis test (SAS Institute Inc., 1999b) was performed to evaluate the significance of the 23 variables measuring postfire infiltration, soil, and vegetation conditions, with the factor being burn severity at the three levels of low, moderate and high. Medians and ranked mean scores for all variables were calculated at the three burn severity levels. Variables that had a  $p$ -value  $\leq 0.05$  were considered significant for determining burn severity.

The nonparametric correlation analysis with the Spearman test (SAS Institute Inc., 1999a) was performed to determine the correlation between the WDPT and infiltrometer

test results. Correlation coefficients were obtained for data in individual burn severity classes and for data pooled from all three burn severity classes. In addition, correlation analysis was also made between those variables significantly affected by burn severity and the water repellency (WDPT and infiltrometer) variables using the pooled data.

Correlations were regarded significant at a  $p$ -value  $\leq 0.05$ .

## **Results and Discussion**

### *Verification of the preliminary BAER burn severity map*

Twenty-one variables measured in the field were tested for significance at each burn severity class. The significant variables were percent mineral soil cover, percent litter cover, percent new litter cover, litter and new litter depth, surface OM content, aspect, the number of live and completely black trees within a 7-m radius, small coarse woody debris, and shrubs (Table 1). Litter cover and depth and the number of shrubs decrease with increasing burn severity due to the combustion of vegetation during the fire. As burn severity increases, percent bare mineral soil cover increases along with percent ash cover. The number of completely black trees within a 7-m radius increases with burn severity, while the number of live trees is lowest at the high burn severity class. One variable that indicates moderate burn severity by the BAER teams is needles remaining on partially burned trees. For this reason, new litter (postfire needlecast) cover and depth was shown to be the highest in the moderate burn class. Organic matter was the lowest at the moderately burned sites and highest at the low burn sites.

Topography can influence burn severity because slope steepness and aspect affect fire spread as well as available fuel. South aspects tend to be drier and therefore more sparsely vegetated, resulting in less fuel and a shorter residence time for fire. Alternatively, north aspects are more densely vegetated and tend to burn longer and hotter, which typically leads to higher burn severity. In this study, the aspect was significantly different at the different burn severity classes (Table 1). Considering all soil, vegetation, and topography variables, about half are significant for determining site burn severity. The characteristics of the ground-measured burn severity variables were reasonably consistent with the remotely-assigned BAER burn severity classes.

#### *Water repellency by burn severity classes*

The mean score of the WDPT (110) for the moderate burn severity class was significantly greater than the mean scores of the low (83) and high (82) severity classes ( $p$ -value 0.004, Table 1). Higher WDPT values indicate increasing water repellency. Soil water repellency was much more persistent in the moderately burned sites. In Figure 2c, the peak at 300 s (skewness -0.1) shows 25 out of 59 plots were in the high water repellency category (WDPT greater than 180 s). At low burn severity (Figure 2a), a skewness of 0.4 indicates that fewer plots were in the high water repellency range. Within the high burn severity plots (Figure 2e), 24 out of 60 plots exhibited low water repellency (WDPT less than 60 s).

The differences in infiltrometer test values were not significant among low, moderate, or high burn severity classes ( $p$ -value 0.06, Table 1). The mean scores suggest

that the infiltration rate was lower for the moderately burned sites, similar to the WDPT test results. Lower infiltration values indicate a higher degree of water repellency. In Figure 2d, moderate burn severity, the sharp peak of values was at the lowest end of the infiltration range (skewness 1.1). In the high burn severity plots (Figure 2f), only two plots indicate high infiltration rates (greater than  $14 \text{ ml min}^{-1}$ ) and low water repellency. The majority of the plots were in the low infiltration range (skewness 1.1).

The strong water repellency in the moderately burned sites on the Hayman Fire was not expected. Water repellency normally increases with increasing burn severity, due to soil heating and complete combustion of surface OM. Moderately burned sites on the Hayman may not have appeared as severely burned (less black), but soil heating could have been longer and deeper, resulting in higher water repellency. The low postfire OM content on the moderately burned sites relative to the high and low burned sites (Table 1) also supports this explanation. On the Hayman Fire, 70 percent (42 out of 60) of the high burn severity plots were in an area that burned very quickly. The fire spread maps indicate that the fire may have moved through this area in less than 30 minutes on the second day of the fire, which was also the day of the greatest spread (Finney *et al.*, 2002). The rapid movement of fire may have resulted in limited soil heating. The lack of soil heating appears to support our finding that there was less water repellency in the high burn severity sites.

### *Correlation of WDPT and Infiltrometer*

The WDPT and infiltrometer tests were strongly correlated at a value of  $-0.65$  ( $p$ -value  $<0.0001$ ) for the pooled data (Table 2). For data grouped by burn severity, the correlation coefficients were  $-0.57$  ( $p$ -value  $<0.0001$ ) for the low severity sites,  $-0.66$  ( $p$ -value  $<0.0001$ ) for the moderate severity sites, and  $-0.70$  ( $p$ -value  $<0.0001$ ) for the high severity sites. The high correlations between classes as well as the high overall correlation suggest compatibility between the two tests. Thus, the presence of water repellent soils may be detected and measured using both tests with reasonable agreement.

The infiltrometer test has the potential to provide additional information about the hydrologic condition of the soil. If cumulative infiltration measurements are made over a period of time, the infiltrometer values can theoretically be converted to soil hydraulic conductivity (Decagon Devices, Inc., 1998). One unsolved problem with the infiltrometer is that the often highly wettable surface layer initially allows lateral infiltration. The infiltration rates may be high until the surface layer is saturated and the wetting front reaches the water repellent soil layer below.

### *Correlation of WDPT and infiltrometer tests to other variables*

Both the WDPT and infiltrometer tests were significantly correlated with other burn severity variables (Table 2), including mineral soil cover ( $-0.29$  and  $0.16$ , respectively) and percent ash cover ( $0.34$  and  $-0.35$ , respectively). Water repellency increased with decreasing soil cover and increasing ash cover. The number of live trees in the surrounding area (7-m radius) was also significantly correlated with both WDPT and

infiltrometer tests, 0.30 and -0.16, respectively. Water repellency decreases when more live trees are present.

WDPT values were highly correlated to ash cover (0.34) and litter depth (0.18) while infiltrometer values were not (Table 2). Infiltrometer results were highly correlated to new litter cover (-0.16) while the WDPT was not. The variables that were significantly correlated with the water repellency tests were also determined to be essential for determining soil burn severity. Therefore, measuring roughly 12 soil and vegetation variables and performing the WDPT or infiltrometer test can classify site burn severity faster and more quantitatively than before.

## **Conclusion**

Based on the soil and vegetation indices measured in the field, the burn severity classes that were initially assigned by the BAER teams seemed appropriate. About half of the variables measured in the burn area were significant for determining burn severity. Many of these variables also had a significant relationship with soil water repellency. By measuring key soil and vegetation factors, along with the WDPT or infiltrometer test, site burn severity and water repellency can be adequately determined. On the Hayman Fire, soil water repellency did not increase with increasing burn severity, as expected. The moderately burned sites exhibited the strongest and most consistent water repellency, according to both WDPT and infiltrometer tests. This was likely due to slow soil heating and nearly complete combustion of surface OM. The high burn severity sites did not exhibit as strong water repellency as expected probably because of the speed at which the

fire traveled through many of the high severity plots. Soil heating was most likely not very deep or at a high enough temperature for strong water repellency to occur. Both WDPT and infiltrometer tests indicated similar water repellency results within each burn severity class. The WDPT and infiltrometer values were strongly correlated at each individual burn severity class as well as overall. The two tests were shown to be compatible and should be used to complement each other. The WDPT is a traditional protocol but only provides infiltration information about a single water drop. The infiltrometer is easier to use in the field than the WDPT, is less subjective, more quantitative, and may be able to provide additional hydrologic information about the soil. Knowing more about the infiltration capabilities of the soil after a fire, such as the relative volume and rate of infiltration that the mini-disk infiltrometer can provide, would be valuable for postfire erosion potential analysis.

### **Acknowledgements**

We thank two independent reviewers for their very helpful comments and suggestions. Special thanks to the field crews in Colorado during the summer of 2002 for their help collecting data. This research was supported by the USDA Forest Service Rocky Mountain Research Station and the USDA and USDI Forest Service Joint Fire Science Program as well as the NSF Integrative Graduate Education and Research Training (IGERT) grant under NSF grant DGE-9972817 to the Center for Multiphase Environmental Research at Washington State University.

**Commercial Product Disclaimer**

The use of trade, firm, or corporation names in this publication is for the information and convenience of the reader. Such use does not constitute an official endorsement or approval by Washington State University or the United States Department of Agriculture of any product or service to the exclusion of others that may be suitable.

## References

- Cipra JE, Kelly EF, MacDonald L. 2002. Part 3: Historical (Pre-1860) and Current (1860-2002) erosion/sedimentation events, key soil properties of the Hayman landscape and their relation to aquatic and terrestrial systems and to rehabilitation activities. In: Graham RT (tech. ed.), *Interim Hayman Fire Case Study Analysis*, US Department of Agriculture Forest Service, Rocky Mountain Research Station, Ft. Collins, CO; 172–178.
- Clothier BE, Vogeler I, Magesan GN. 2000. The breakdown of water repellency and solute transport through a hydrophobic soil. *Journal of Hydrology* **231–232**: 255–264.
- Colorado Climate Center. 2002.  
<http://climate.atmos.colostate.edu/dataaccess.shtml> [2003, January]
- DeBano LF, Savage SM, Hamilton DA. 1976. The transfer of heat and hydrophobic substances during burning. *Soil Science Society of America Journal* **40**: 779–782.
- DeBano LF. 2000a. Water repellency in soils: a historical overview. *Journal of Hydrology* **231–232**: 4–32.
- DeBano LF. 2000b. Review: The role of fire and soil heating on water repellency in wildland environments: a review. *Journal of Hydrology* **231–232**: 195–206.
- Decagon Devices Inc. 1998.  
<http://www.decagon.com/instruments/infilt.html> [2003, June]
- Dekker LW, Ritsema CJ. 1994. How water moves in a water repellent sandy soil 1. Potential and actual water repellency. *Water Resources Research* **30**: 2507–2517.
- Finney MA, McHugh CW, Close K. 2002. Fire behavior, fuel treatments, and fire suppression team report. In: Graham RT (tech. ed.), *Interim Hayman Fire Case Study Analysis*, US Department of Agriculture Forest Service, Rocky Mountain Research Station, Ft. Collins, CO; 45–57.
- Giovannini G, Lucchesi S. 1997. Modifications induced in soil physio-chemical parameters by experimental fires at different intensities. *Soil Science* **1627**: 479–486.
- Huffman EL, MacDonald LH, Stednick JD. 2001. Strength and persistence of fire-induced soil water repellency under ponderosa and lodgepole pine, Colorado Front Range. *Hydrological Processes* **15**: 2877–2892.
- Jain TB. 2002. Burn severity analysis data form. Unpublished study plan. USDA Forest Service Rocky Mountain Research Station, Moscow, ID.

- Letey J. 2001. Causes and consequences of fire-induced soil water repellency. *Hydrological Processes* **15**: 2867–2875.
- Letey J, Carillo MLK, Pang XP. 2000. Review: Approaches to characterize the degree of water repellency. *Journal of Hydrology* **231–232**: 61–65.
- Nishita H., Haug RM. 1972. Some physical and chemical characteristics of heated soils. *Soil Science* **113**: 422–430.
- Parsons A. 2003. Burned area emergency rehabilitation (BAER) soil burn severity definitions and mapping guidelines. Unpublished report. USDA Forest Service Remote Sensing Application Center, Salt Lake City, UT.
- Pierson FB, Robichaud PR, Spaeth KE. 2001. Spatial and temporal effects of wildfire on the hydrology of a steep rangeland watershed. *Hydrological Processes* **15**: 2905–2916.
- Remote Sensing Applications Center. 2003. Burned Area Emergency Rehabilitation (BAER) Imagery Support.  
<http://www.fs.fed.us/eng/rsac/baer/> [2003, May]
- Robichaud PR. 2000. Fire effects on infiltration rates after prescribed fire in Northern Rocky Mountain forests, USA. *Journal of Hydrology* **231–232**: 220–229.
- Robichaud PR, Beyers JL, Neary DG. 2000. *Evaluating the effectiveness of postfire rehabilitation treatments*. Gen. Tech. Rep. RMRS-GTR-63. USDA Forest Service, Rocky Mountain Research Station, Ft. Collins CO; 85p.
- Robichaud PR, MacDonald L, Freeouf J, Neary D, Martin D. 2002. Postfire Rehabilitation. In: Graham RT (tech. ed.), *Interim Hayman Fire Case Study Analysis*, US Department of Agriculture Forest Service, Rocky Mountain Research Station, Ft. Collins, CO; 241–262.
- Romme WH, Veblen TT, Kaufmann MR, Regan CM. 2002. Ecological Effects Part 1: Historical (Pre-1860) and current (1860 to 2002) fire regimes of the Hayman landscape. In: Graham RT (tech. ed.), *Interim Hayman Fire Case Study Analysis*, US Department of Agriculture Forest Service, Rocky Mountain Research Station, Ft. Collins, CO: 151–156.
- Ryan KC, Noste NV. 1983. Evaluating prescribed fires. In: Lotan JE, Kilgore BM, Fischer WC, Mutch RW (tech. coords.) *Proceedings, symposium and workshop on wilderness fire*. Gen. Tech. Rep. INT-182. US Department of Agriculture, Forest Service, Intermountain Research Station, Ogden, UT: 230–238.

- SAS Institute Inc. 1999a. *SAS/STAT<sup>®</sup> User's Guide, Volume 1, Version 8.2*. Statistical Analysis Systems (SAS) Institute Inc., Cary, NC.
- SAS Institute Inc. 1999b. *SAS/STAT<sup>®</sup> User's Guide, Volume 2, Version 8.2*. Statistical Analysis Systems (SAS) Institute Inc., Cary, NC.
- SAS Institute Inc. 1990. *SAS Procedures Guide, Version 6, 3<sup>rd</sup> edition*. Statistical Analysis Systems (SAS) Institute Inc., Cary, NC.
- Savage SM, Osborn J, Letey J, Heaton C. 1972. Substances contributing to fire-induced water repellency in soils. *Soil Science Society of America Proceedings* **36**: 674–678.
- Shakesby RA, Doerr SH, Walsh RPD. 2000. The erosional impact of soil hydrophobicity: current problems and future research directions. *Journal of Hydrology* **231–232**: 178–191.
- Smith RT, Atkinson K. 1975. *Techniques in Pedology: a handbook for environmental and resource studies*. Elek, London; 213p.
- USFS. 2002. Burned Area Report.  
[http://wildfiresw.nwcg.gov/colorado/baer/hayman\\_fire\\_BAER\\_final.htm](http://wildfiresw.nwcg.gov/colorado/baer/hayman_fire_BAER_final.htm) [2003, April]
- Wang Z, Wu QJ, Ritsema CJ, Dekker LW, Feyen J. 2000. Effects of soil water repellency on infiltration rate and flow instability. *Journal of Hydrology* **231–232**: 265–276.
- Zhang R. 1997. Determination of soil sorptivity and hydraulic conductivity from the disk infiltrometer. *Soil Science Society America Journal* **61**: 1024–1030.

Table 1. Water repellency tests, ground cover, vegetation, and topography variables in order of their significance for determining burn severity ( $n=182$ ). All variables are measured within a 4-m plot unless otherwise specified. Medians are listed first at each burn severity class and mean scores are in parentheses. Variables are significant at a  $p$ -value  $\leq 0.05$  for determining burn severity.

Variables	Burn Severity Classes			$p$ -value	Significant
	Low	Moderate	High		
<b>Water Repellency Tests</b>					
WDPT (s)	103 (83)	168 (110)	107 (82)	0.004	Y
Infiltrometer ( $\text{ml min}^{-1}$ )	4.8 (101)	3.3 (79)	4.0 (94)	0.06	N
<b>Ground Cover Characteristics</b>					
Mineral soil exposed (%)	11 (67)	32 (89)	65 (122)	<0.0001	Y
Litter cover (%)	49 (116)	37 (106)	10 (54)	<0.0001	Y
Litter depth (mm)	6 (114)	4 (109)	1 (54)	<0.0001	Y
New litter cover (%)	2 (106)	8 (117)	1 (53)	<0.0001	Y
New litter depth (mm)	1 (101)	1 (111)	0 (65)	<0.0001	Y
Surface soil organic matter (%)	4.5 (97)	2.9 (71)	4.4 (93)	0.01	Y
Humus depth (mm)	0 (88)	0 (96)	0 (94)	0.08	N
Rock cover (%)	0 (96)	0 (82)	0 (99)	0.08	N
Ash cover (%)	10 (85)	10 (89)	16 (104)	0.12	N
Humus cover (%)	0 (89)	0 (95)	0 (95)	0.20	N
<b>Vegetation Characteristics</b>					
Coarse woody debris ( $d < 80$ mm) (%)	2 (114)	2 (94)	1 (68)	<0.0001	Y
Black trees in 7-m radius (count)	0 (72)	0 (79)	3 (124)	<0.0001	Y
Shrubs (#)	0 (88)	0 (85)	0 (105)	0.01	Y
Trees in 7-m radius (#)	6 (97)	5 (101)	4 (77)	0.03	Y
New grasses (%)	1 (102)	1 (90)	1 (85)	0.05	N
New forbs (%)	0 (89)	1 (103)	0 (85)	0.09	N
Stumps (%)	0 (91)	0 (99)	0 (87)	0.14	N
Coarse woody debris ( $d > 80$ mm) (%)	0 (98)	0 (87)	0 (92)	0.44	N
Burned cubical material (%)	0 (94)	0 (92)	0 (91)	0.91	N

**Topographical Characteristics**

Aspect (degree)	210 (95)	210 (104)	108 (78)	0.02	Y
Slope (%)	14 (94)	15 (93)	10 (89)	0.82	N

---

Table 1 cont.

Table 2. Correlation between significant burn severity variables and water repellency test variables. The first number is the correlation coefficient and the number in parenthesis is the *p*-value. Significant test results are in bold.

<b>Variables</b>	<b>WDPT</b>	<b>Infiltrometer</b>
WDPT	1.0	<b>-0.65 (&lt;0.0001)</b>
Infiltrometer	<b>-0.65 (&lt;0.0001)</b>	1.0
Mineral soil exposed (%)	<b>-0.29 (0.0001)</b>	<b>0.16 (0.04)</b>
Litter cover (%)	0.14 (0.07)	-0.007 (0.92)
Litter depth (mm)	<b>0.18 (0.02)</b>	-0.03 (0.68)
New litter cover (%)	0.12 (0.13)	-0.16 ( <b>0.04</b> )
New litter depth (mm)	0.04 (0.60)	-0.10 (0.21)
Surface soil organic matter (%)	0.14 (0.06)	-0.14 (0.07)
Ash cover (%)	<b>0.34 (&lt;0.0001)</b>	<b>-0.35 (&lt;0.0001)</b>
Trees in 7 m radius (#)	<b>0.30 (&lt;0.0001)</b>	<b>-0.16 (0.04)</b>
Black trees in 7 m radius (#)	0.12 (0.13)	-0.11 (0.14)

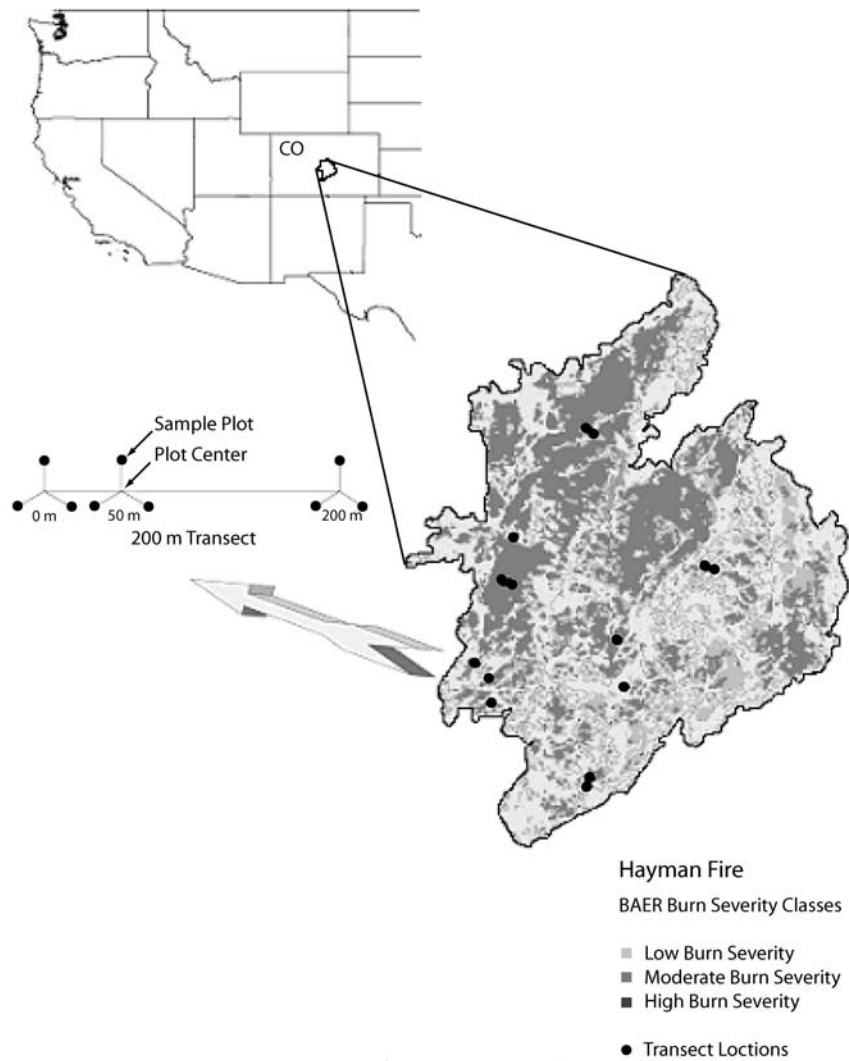


Figure 1. Hayman Fire location in Colorado, sample plot locations within the fire, and the transect layout.

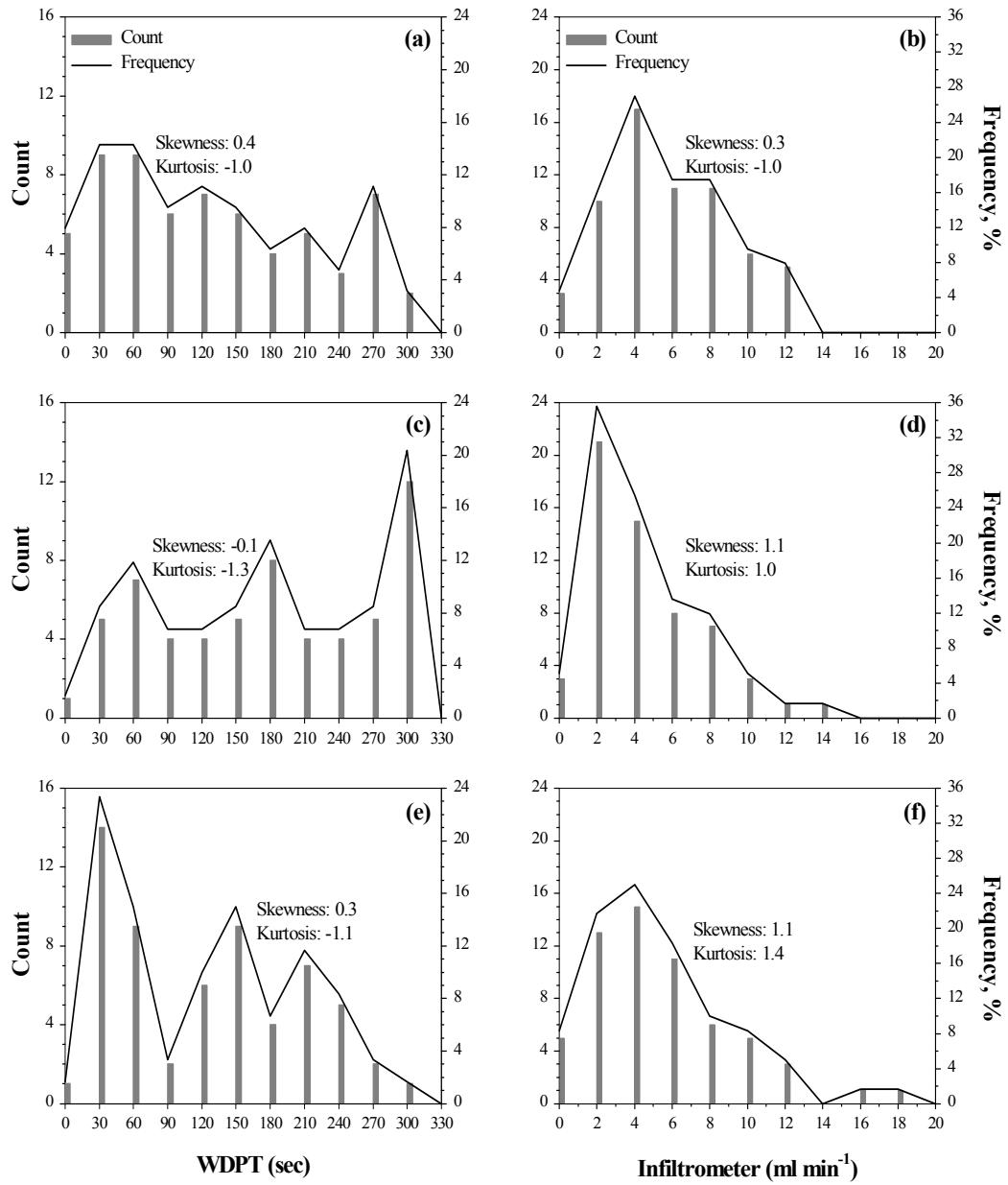


Figure 2. Distribution of water repellency measurements at low ( $n=63$ ) (a, b); moderate ( $n=59$ ) (c, d); and high ( $n=60$ ) (e, f) burn severities. Graphs (a), (c), and (e) are WDPT values and graphs (b), (d), and (f) are infiltrometer values.

## CHAPTER THREE

### HYPERSPECTRAL REMOTE SENSING OF WATER REPELLENT SOILS

#### AFTER THE HAYMAN FIRE, COLORADO

Sarah A. Lewis, Joan Q. Wu, Peter R. Robichaud, Bruce E. Frazier and William J. Elliot

#### **Abstract**

The remote detection of soil erosion potential after forest fires would lead to quicker and more accurate erosion mitigation. There is a change in the organic properties of soil after a fire that often leads to a water repellent layer being formed, which results in decreased soil infiltration capacity. The erosion potential of soil can be estimated *in situ* with several different tests, all of which require an extensive amount of time to evaluate a large fire. Many soil properties, including soil organic matter, can be measured remotely. Remote sensing is increasingly being used for environmental risk assessment, and postfire erosion potential is a new application. By remotely quantifying measurable soil properties, a link can be made to the soil's hydrologic condition and the possibility of erosion can be predicted. A hyperspectral image was acquired over the Hayman Fire in the summer of 2002 and ground data were collected measuring the infiltration capabilities of the soil. A supervised classification was run on the image in an attempt to identify soils that were highly water repellent and therefore high risk for erosion. The classification was not accurate in determining water repellency severity, but it was nearly 80 percent accurate for identifying the presence of water repellency. According to the classified images, nearly 20

percent of the Hayman Fire was at a high risk for erosion, and mitigation should be focused on these areas.

## **Introduction**

Collecting timely information about post-wildfire soil conditions is among the most urgent and important tasks for determining postfire erosion potential and recommending mitigation measures. The hydrologic condition of soil typically deteriorates considerably after a fire; infiltration capabilities decrease and erosion potential increases (Letey, 2001; DeBano, 2000a; Robichaud, 2000). Much of the decrease in infiltration can be attributed to the formation of water repellent soils after a moderate or high intensity fire (DeBano, 2000a; Giovannini and Lucchesi, 1997; DeBano *et al.*, 1976).

Fires that have long residence time and reach high temperatures (175–280°C) often volatilize the surface organic layer and render the soil water repellent (Letey, 2001; DeBano, 2000b). As the organic compounds cool, they form a hydrophobic layer around individual soil particles (DeBano *et al.*, 1976). The formation of this non-continuous hydrophobic layer generally occurs at or below the soil surface, up to five cm in depth (Clothier *et al.*, 2000; DeBano, 2000b). Soil water repellency is highly spatially variable, thus, the non-continuity will occur laterally, as well as vertically within the soil profile. The vertical component is generally dependent on the soil heat gradient of the fire; higher soil temperatures often lead to the formation of water repellent soils. The depth and severity of water repellency depends on the pre-fire conditions, especially soil moisture and available fuel, and the temperature and duration of the fire (Robichaud and

Hungerford, 2000). Soils with low antecedent moisture and high organic matter (OM) contents subjected to a high temperature fire that burns slowly will likely become highly water repellent.

There are several tests currently used in the field to test for the presence and severity of water repellent soils: water drop penetration time (WDPT), critical surface tension (CST) or a new, mini-disk infiltrometer test (Lewis *et al.*, 2003, in review; DeBano, 2000b; Letey *et al.*, 2000). The physical basis of these tests is the approximation of the soil-water contact angle; water repellent soils are those with a contact angle greater than or equal to 90 degrees (Letey *et al.*, 2000). The WDPT approximates the soil-water contact angle through the measurement of the time that a water drop will remain on the soil surface without infiltration. With this technique, a soil is characterized as water repellent if a water drop placed on the soil surface does not infiltrate within five seconds (DeBano, 2000a; Letey *et al.*, 2000). The CST method measures the soil-water contact angle more precisely than the WDPT through the application of increasing concentrations of aqueous ethanol solutions. Higher ethanol concentrations have a lower surface tension; thus, severely repellent soils will only be infiltrated by a high-concentration ethanol solution (Huffman *et al.*, 2001; Letey *et al.*, 2000).

The mini-disk infiltrometer test measures the volume of water that infiltrates into the soil in the first minute. Low infiltration rates indicate high surface water repellency and consecutive infiltrometer measurements can theoretically be used to calculate soil hydraulic conductivity (Decagon Devices Inc., 1998; Zhang, 1997). The infiltrometer test takes half the time of the WDPT and the subjectivity has been greatly reduced. One

problem with the infiltrometer, however, is that the wettable surface layer frequently allows lateral infiltration. The infiltration rate may be high initially until the surface is saturated and the wetting front reaches the water repellent layer. *In situ* sampling for water repellent soils is time consuming and subjective, and current methods are not adequate for sampling on a large spatial scale.

Forest fires often cover large areas (greater than 50,000 ha) and the limitations of the aforementioned tests are further exacerbated when used to classify water repellency on these large fires. Because of the time required and inconsistency between testers with the current water repellency tests, the need for alternative methods that do not require intensive manual sampling becomes evident. Remote sensing is a promising possibility, as the sampling can be performed remotely rather than on-site. If it were possible to make reliable predictions from a remote sensor (satellite or aircraft-mounted), larger burned areas could be evaluated in less time than is required to test with the *in situ* methods. Ground samples would still be required to validate the remotely sensed data, but far fewer samples would be necessary.

Numerous remote sensing methods are currently used for gathering geo-information in the field. Passive remote sensors, such as hyperspectral remote sensors, measure electromagnetic energy that is naturally reflected or emitted (Jensen, 1996). A passive sensor generates a spectral image, with the number of spectra being measured and recorded dependent on the capabilities of the sensor. Multi-spectral and hyperspectral remote sensing instruments collect between three and several hundred bands of spectral data at one time (Jensen, 1996). The data resolution (spatial and spectral) also depends on

the capabilities of the sensor. An instrument that collects hundreds of continuous, narrow wavebands provides a greater array of data than a sensor that collects only a few broad bands.

There are many applications of remote-sensing techniques to the measurement of environmental features. Spectral remote sensing is useful for detecting vegetation types, land covers, soil water content, OM content, soil texture and soil mineral content (Chang and Islam, 2000; Jackson and LeVine, 1996; Jackson *et al.*, 1995). Vegetation type and condition can be remotely sensed, particularly in the near-infrared (NIR) region of the spectrum (Patterson and Yool, 1998). Soil texture and type, and moisture and OM content are measurable remotely with high-resolution instruments (Chang and Islam, 2000; Palacios-Orueta and Ustin, 1998; Jackson and LeVine, 1996; Coleman and Montgomery, 1987). Water's highly electric properties make it possible to detect remotely whether in soil or on the surface. Many of these remotely detectable soil properties are changed after a fire; soil texture becomes finer and soil moisture and OM content decreases (Giovannini and Lucchesi, 1997; Nishita and Haug, 1972). By measuring identifiable soil properties remotely, water repellency will likely be detectable and possibly quantifiable. It is expected that water repellent soils with low surface OM content due to burning will have a distinctive spectral reflectance when compared a soil that is not water repellent and has higher surface OM content. Soil with high OM content is generally dark in color and is less reflective in the visible region than soil with low OM content (Sudduth and Hummel, 1991; Henderson *et al.*, 1989).

Additionally, soil having burned OM contains aliphatic hydrocarbons (Schmid *et al.*, 2001; Almendros *et al.*, 1990; Savage *et al.*, 1972). These hydrocarbons have been identified in water repellent soils after forest fires, due to the burning of OM (Savage *et al.*, 1972). An abundance of aliphatic functional groups in a burned soil may suggest water repellent soil conditions due to the quantity of OM combusted during the fire. The aliphatic hydrocarbons in burned soil should be detectable using the high-spectral resolution instruments in the lab as well as in the field. The region from 1400 to 2100 nm (near-infrared and short wave infrared) experiences significant absorption by many organic compounds (Fidencio *et al.*, 2002; Hummel *et al.*, 2001; Ben-Dor and Banin, 1995; Henderson *et al.*, 1992). The waveband centers 2215, 2265, 2290 nm, and the range 2315-2495 nm were identified by Henderson *et al.* (1992) to be useful for identifying the presence of organic substances, as were the bands 1585, 2017, and 2388 nm, identified by Ben-Dor and Banin (1995). These wavebands were analyzed closely for variations between the water repellency classes.

Applications of remote sensing to forest fire studies is becoming standard practice. The development of a postfire soil burn severity map is generally the first step in postfire assessment after a large fire (Remote Sensing Applications Center, 2003). The reflectance spectra from a satellite multispectral image such as LANDSAT or SPOT (Systeme pour l'Observation de la Terre) are used to create a classification of increasing soil burn severity, and the resulting potential for erosion (Remote Sensing Applications Center, 2003). Although the images from these satellites are inexpensive (or free) the data have low spatial and spectral resolution. The maps which are generated from these images are

intended to be used for quick assessment of fire-induced changes to surface conditions which may increase erosion and runoff (Parsons, 2003, unpublished report). The spatial accuracy of low-resolution burn severity maps as well as the applicability of the maps to diverse environments has been questioned. Multi-spectral data have been used for several years with reasonable success, yet the recent accessibility of hyperspectral images with their high spatial and spectral resolution has allowed for new mapping techniques and applications to be explored. High quality, remotely sensed fire maps can provide valuable information about the postfire soil and vegetation conditions, and allow for more accurate and effective erosion mitigation.

A comprehensive USDA Forest Service Rocky Mountain Research Station project is underway on the Hayman Fire in central Colorado to explore methods of determining burn severity and soil water repellency remotely in order to expedite the identification of high-risk areas for soil erosion. The two-year project is funded by the Joint Fire Science Program. Hyperspectral imagery and ground data were collected in August 2002. The first portion of the study has recently been completed, which was focused on the analysis of the ground data, the comparison of the WDPT and mini-disk infiltrometer for determining water repellency, and the relationship between soil burn severity and water repellency (Lewis et al., 2003). The study found that the WDPT and mini-disk infiltrometer tests were highly correlated and that on the Hayman Fire, water repellency was greatest within the moderate burn severity classified areas. The sample plots with a high degree of water repellency were found mostly in the areas that were initially classified as moderately burned by the Burned Area Emergency Rehabilitation (BAER) map.

The primary goal of this study is to examine hyperspectral remote sensing techniques as a potential tool for rapidly and efficiently determining soil water repellency. It is anticipated that water repellent soils will have unique spectral signatures and possibly the spectral detection of aliphatic hydrocarbons will provide indicators that are associated with water repellent soils. The specific objectives are: (1) to determine whether organic properties of the study soils are identifiable spectrally and whether there is a difference between low, moderate, and high water repellency soils based on these organic spectral features; (2) to determine which wavelengths(s) have the strongest correlation with water repellent soils; and (3) to use water repellency ground data to run a supervised classification on two typical flight lines of hyperspectral data obtained on the Hayman Fire.

## **Methods and Materials**

### *Study Area*

The Hayman Fire burned on the Pike and San Isabelle National Forests in central Colorado (Figure 1). The fire started in early June and burned nearly 60,000 ha by the end of August of 2002. The Hayman Fire was the largest in Colorado fire history. Across the fire site, 31 percent of the total area was initially classified as low severity by the BAER team soil burn severity map, 20 percent as moderate burn severity, 32 percent as high burn severity, and 17 percent was unburned (USFS, 2002). The elevation ranges from 1,700 m at the base of the fire to about 3,600 m within the fire perimeter and the slopes range between 10 and 50 percent. The region is semi-arid, with a late summer monsoon season

that often delivers short-duration, high-intensity storms. An average of 500 mm of precipitation falls annually with average winter temperatures around 0°C and average summer temperatures about 20°C (Colorado Climate Center, 2002).

The dominant canopy vegetation is Ponderosa pine (*Pinus ponderosa*) and Douglas fir (*Pseudotsuga menziesii*) with Aspen (*Populus tremuloides*) groves in the lower elevations near water. The mostly granitic soils (Sphinx and Legault) are underlain by the Pikes Peak batholith, with frequent rocky outcroppings (USFS, 2002). Sandy loams, gravely sandy loams, and clay loams make up the remaining soils within the fire perimeter (Graham, 2003). Although unknown exactly, the pre-fire OM content of the soil for the majority of the burn area was believed to be relatively low. For the purpose of the image analysis, these soils will be referred to as granitic soils to distinguish between the soils on which the water repellency tests were performed (sometimes below the ash and litter) and the soil percent cover category that is used to classify the ground truth plots. For a more detailed description of the vegetation and soils, see Lewis *et al.* (2003) or The Hayman Fire Case Study Analysis (Graham, 2003).

### *Sampling Scheme*

A target of sixty sample points were selected in each of the three burn severity classes following the BAER soil burn severity map (low, moderate, and high) for a total of 182 sample points. Points were positioned along east-west transects that were 200 m in length (Figure 1). Each transect endpoint (locations 0 and 200 m) as well as the point 50 m from the west endpoint were referred to as central reference points. Extending from each

central point were three 20-m radials in the azimuthal directions 0, 120 and 240 degrees, respectively. The actual sample points were located at the end of each of these radials. Each sample point was a 4-m diameter circle in which all water repellency measurements were made. In order to locate sample points on the image, GPS coordinates were collected at least two times on each transect. For accuracy, 100 points were collected at each location for position averaging. Differential correction was performed using base station data from Compasscom, Inc., Denver, CO.

#### *Water Repellency Tests*

The WDPT test was replicated 11 times along a 50-cm line transect within each 4-m circle. Surface ash and litter were carefully removed to reveal the bare mineral soil. Water repellency was divided into three classes by the average time to water drop infiltration per plot: low repellency (6–60 s), moderate (61–180 s), and high (181–300 s). These water repellency classes are generally based on the classes outlined by Dekker and Ritsema (1994).

On a line parallel to and within 200 mm directly above or below the WDPT test line, four infiltrometer tests were performed. The mini-disk infiltrometer was filled with water and placed on the soil surface at four evenly spaced locations along the line. The time to the start of infiltration was noted, as was the volume of water that infiltrated into the soil within the first minute of infiltration.

### *Organic Matter Determination*

A loss on ignition (dry combustion) procedure (Smith and Atkinson, 1975) was performed on all soil samples taken from the 182 sampling points to determine the OM content. Soil samples were oven-dried at 105° for 24 hours to remove moisture and then transferred to a muffle furnace for combustion at 375°C for 16 hours. Theoretically, all OM should have been volatilized in this procedure, and after cooling to room temperature, the percent soil OM was calculated by mass.

### *Aerial remote sensing*

A Probe-2 hyperspectral sensor (Earth Search Sciences Inc., Kalispell, MT) was mounted to a fixed-wing aircraft for hyperspectral data collection over the Hayman Fire in August 2002. Fourteen flight lines were flown for continuous coverage of the fire site and the elevation of the sensor was 7,000 m above the ground. The sensor measures reflectance at a high spectral resolution over the range of 400–2500 nm. The spectral resolution of the data in the visible range (400–700 nm) as well as the NIR (700–1400 nm) and the SWIR (short-wave infrared, 1400–2500 nm) range was 15 nm, resulting in 128 bands of data. The spatial resolution of the processed data was 5.1 m. As each of the on-ground plots was a 4-m circle, each plot was considered one pixel in the image analysis.

### *Field Spectrometry*

*In situ* reflectance measurements were made at high and low burn severity areas using a hand-held hyperspectral sensor (Analytical Spectral Devices, Boulder, CO). A total

of 330 readings were taken at seven different sites. Three sites each of high burn severity and low burn severity above-canopy measurements were sampled to help set apart the effect of the canopy on soil reflectance. At one high burn severity site, soil reflectance measurements were taken just above the soil surface in an attempt to collect a high burn severity soil endmember. Above-canopy measurements were taken in a bucket truck capable of extending 15 m above the ground. The sensor was moved around within the canopy for the duration of the measurement in both black and live canopies.

### *Image Pre-processing*

Pre-processing of the image data consisted of radiometric correction from the raw digital numbers using calibration reference points to standardize the data. The radiance data were converted to reflectance by an atmospheric modeling algorithm combined with spectral and ground data from the scene. Specifically, the Hayman image data was converted to reflectance using the atmospheric modeling algorithm Atmosphere Removal program (ATREM) (University of Colorado, 2003). The reflectance data were analyzed for over- or under-correction (spiky values or negative values) using procedures built into typical hyperspectral software packages.

Geo-rectification was performed within Environment for Visualizing Images (ENVI) software using input geometry (IGM) files provided with the reflectance data. The IGM files contained reference information about every pixel and placed pixels in user-defined coordinate space. In ENVI, IGM files were used to create geographic lookup tables (GLTs) that determine which input pixel will occupy a specific location as an output pixel.

Once the GLT was built, it was applied to the reflectance data, and the result was an image file with corrected map coordinates (UTM, zone 13N). Finally, the ground truth plots were located on the image using the GPS coordinates that were collected at each site.

### *Principal Component Transform*

A principal component (PC) transform was performed on the reflectance data in order to identify the major source(s) of variance in the image as well as to reduce the dimensionality of the hyperspectral data (Richards and Jia, 1999; Jensen, 1996). Hyperspectral data are often highly correlated due to the high spectral resolution. The principal component transform maximizes the variance in just a few bands of data and results in uncorrelated output bands. In order to identify the most useful NIR and SWIR data, the PC transform was performed on reflectance data between 1482 and 2451 nm, and 20 output PC bands were generated. Generally, the first three PC bands contain 95 percent of the variance in the image (Patterson and Yool, 1998) and the first 10 bands contain 99.9 percent of the variance. On both FL4 and FL7, PC bands 1-3 contain 99.9% of the variance and bands 1–10 contain nearly 100% of the variance. PC bands 11-20 appeared very noisy and therefore not especially informative on either flight line. On FL4, the first PC band (PC1) was most correlated with SWIR bands 2183–2235 nm and a group of NIR bands 1742–1779 nm. The second PC band (PC2) was associated with SWIR bands 2287-2451 nm, as was the third PC band (PC3). On FL7, PC1 was also most correlated with SWIR bands 2183–2235 nm. PC2 was most correlated with bands 1697 and 1564 nm. PC3 was

most correlated with bands 1717 and 1537 nm. Subsequent image analysis was focused on the first 10 PC bands.

### **Image Classification**

A spectral library of the 182 plots where water repellency data were collected was built. The reflectance at the sample points was analyzed by site and by the water repellency classes of low, moderate, and high. Mean reflectance values for soils in each water repellency class were calculated over the entire spectrum and individual reflectance signatures were visually analyzed for distinctive features. The statistical difference between reflectance values of low, moderate and high water repellency soils was determined waveband by waveband in SAS (SAS Institute Inc., Cary, NC, 1999) with the general linear model procedure.

The mean reflectance values of the low, moderate and high water repellency plots were first visually analyzed for distinct spectral features in the NIR and SWIR range. The visual analysis was done to find out if unique spectral absorbance or reflectance features were present in one severity of water repellent soils and not in another, or if a feature was more or less pronounced in a specific water repellency severity. Wavebands above 1500 nm were also statistically analyzed for correlation between reflectance values and water repellency values or soil OM contents.

Due to the size of the image data set, the majority of the image analysis was performed on two flight lines only, namely flight line 4 (FL4) and flight line 7 (FL7). Fifty plots were on FL4 and 53 plots were on FL7; more than half of the total study plots were

on these two flight lines. On FL4, 22 plots had low water repellency, 16 moderate, and 12 high. On FL7, 12 plots had low water repellency, 23 moderate, and 18 high. On the individual flight lines, regions of interest (ROIs) were built to separate high, moderate and low water repellency plots, which allowed for distinct spectral regions to be separated as training classes (endmembers) for supervised classification (Figure 2). The separability of the ROIs was calculated using the Jeffries-Matusita and Transformed Divergence separability measures in ENVI (Richards and Jia, 1999). The separability output of this test ranged from 0 to 2, with 0 being the least separable and 2 being the most. The three water repellency class ROIs received the highest separability score possible for all combinations of classes. The ROIs were determined to be adequately dissimilar and were therefore acceptable choices for endmembers in the supervised classification. For validation, approximately twenty percent of the plots (4 or 5 plots per water repellency class per flight line) were randomly chosen and excluded when building a second set of endmembers. Due to the small number of validation pixels, a third set of endmembers were built reserving half of the plots for validation. These plots were reserved for the subsequent validation to evaluate the accuracy of the classifications.

In addition to water repellency classes, major features such as water, granitic soil (sand) and green and black canopy vegetation were also used as endmembers in classifications (Figure 3). The PC transformed image was useful for identifying endmembers (Figs 4 and 5). The granitic soil was found to correspond closely with the first PC band, brightness, on both FL4 and FL7, as was also found in Patterson and Yool (1998). The second PC band correlated well with green vegetation and the third band

seemed to have an association with blackness, or the areas that had prevalent charring of the soil and vegetation. Green and black canopy vegetation endmembers were imported into ENVI from the field spectrometry measurements. Green canopy was relatively easy to separate from the surroundings due to its distinct signature; green vegetation stood out well on both the PC image and the RGB image (bands 118, 36, 9) (Figs 4 and 5). The reflectances of green pixels were collected and averaged in several regions on both flight lines in order to build a green vegetation endmember. Back canopy was difficult to visually separate, so the signature from the field spectrometry was used directly in the supervised classification.

An unsupervised classification technique, Iterative Self-Organizing Data Analysis Technique (ISODATA), was applied to the PC images on both FL4 and FL7. ISODATA classification identifies statistical means that inherently exist in the data set and classifies all pixels based on the minimum distance to a mean (ENVI, 2000). All pixels were classified into seven classes in order to draw a relationship to the seven endmember supervised classification that was later run (water, green and black vegetation, bare soil, and low, moderate, and high water repellent soils). Based on the ISODATA classification, a classification matrix was built to determine the separability of the data and whether the separability was associated with the water repellency classes of the soils.

The endmembers previously identified were used as training classes with the PC images for a supervised classification. Spectral Angle Mapper (SAM) calculates the spectral angle in  $n$ -dimensional space between spectra to compute a match to reference spectra or endmembers (ENVI, 2000). The smaller the angle, the better the match. Spectra

that have too large an angle of difference from the endmember spectra (default 0.1 radians) were not classified. Seven endmembers were used in the first SAM classification on both flight lines: water, granitic soil and green and black canopy vegetation, as well as low, moderate, and high water repellency plots. The number of plots classified into each class was calculated as well as the unclassified area and areas assigned to each endmember. Next, the classification was performed with the second and third sets of endmembers, with 20 percent and 50 percent of the water repellency study plots respectively, reserved for post-classification validation. The number of pixels in each class was again calculated and a classification matrix was created for the accuracy assessment of all classifications.

## **Results and Discussion**

### *Mean comparisons*

FL4 and FL7 mean reflectance values were plotted over the entire range of measured wavelengths (400–2500 nm) (Figure 2). The mean reflectance values of the high water repellency plots were significantly different ( $\alpha=0.05$ ) than the reflectance values from low water repellency plots over the entire spectral region when they were analyzed band by band in SAS (Table 1). The mean reflectance values of the high water repellency plots were significantly different from the moderately water repellent plots only over the wavelengths 1510–1791 nm, and only at  $\alpha$  greater than or equal to 0.2; Based on this analysis, these wavelengths were determined to be important for remote identification of soil water repellency. Thus, subsequent analysis focused on the spectral region above 1500

nm. Five water absorption bands around 1900 nm were excluded because of their affect on the overall shape of the spectra.

The average reflectance of the highly water repellent plots was lower than both the moderate and low water repellent plots (Figure 2). The reflectance was lower likely due to the presence of light-absorbing carbon and dark ash (char) on these plots (Clark, 1983). As water repellency increased, the percentage of charred soil also increased; from 27 percent surface cover on the FL4 low water repellent plots to 56 percent surface cover on the high water repellent plots and from 16 percent to 32 percent on the FL7 low and high water repellent plots (Table2). Charring of the light colored, granitic soils produces a much darker and less reflective soil. Ash mixed with soil (especially after a rainfall, such was the case on the Hayman) is dark colored, less reflective, and the two components are not easily discernible. The percent mineral soil cover decreased and the percent of ash increased with increasing water repellency (Table 2), both of which are consistent with the overall reflectance of the high water repellency plots being lower. The percent litter cover increased with increasing water repellency as did the percent of charred litter on each plot. The increase in litter was likely associated with the increase in OM as water repellency increased.

It was initially thought that soil OM would be much less in the high water repellency soils when compared to the low repellency soils. The exact opposite was true; OM increased from 4.4 to 9.7 percent on FL4 and from 4.7 to 5.9 percent on FL7 between the low and high water repellency plots, respectively. The likely explanation is that the soils that became slightly water repellent had very low soil OM prior to the fire and

therefore had very little to volatilize. The fire did not induce the formation of water repellent soils on these sites. The soils with high water repellency had high pre-fire soil OM and therefore more OM to burn and to subsequently become water repellent. Although pre-fire soil water repellency was not known, it is probable that the areas with widespread granitic soils and little surface litter or soil OM were not naturally water repellent.

The reflectance values of the moderate water repellency plots were very similar to those of the low water repellency plots and nearly indistinguishable in certain regions, especially on FL7 (Figure 2). The distinct difference between high water repellency plots versus moderate or low water repellency plots suggested that it may be difficult to quantify the severity of water repellency at multiple levels with this image analysis. However, it may be easier to identify the presence or absence of highly water repellent soils due to the distinct spectral signature.

### *Spectral Features*

A visual comparison of the mean reflectance values of low, moderate, and high water repellent plots showed little difference in absorbent or reflective spectral features (Figure 2). The individual shapes of the low, moderate and high mean spectral signatures were nearly identical within each flight line. A couple of soil and mineral (Aluminum and Iron Hydroxides, AlOH and FeOH) features were visible in the shortwave-infrared region, between 2200 and 2400 nm, especially on the low and moderate water repellency plots of FL4 (Figure 2). The low and moderate water repellent plots on FL4 had 70 percent and 57 percent soil exposure, respectively. These soil mineral features were present at all three

levels of water repellency; however, they appeared to have less depth (less pronounced) in the highly water repellent soils. The dampening of the features was likely due to the presence of the dark ash and carbon in the areas of high burn severity (Clark, 1983). The wavebands previously identified by Henderson et al. (1992) and Ben-Dor and Banin (1995) as important for OM analysis were inconsequential in this case. The individual wavebands were not statistically correlated with either the water repellency measurements or the OM contents of the respective plots. There were no features that are significantly different at one class of water repellency versus any other class in the NIR or SWIR spectral regions. Again, it is likely that if absorption features were present that they were dampened by the prevalent blackness from the fire.

#### *Unsupervised classification*

The ISODATA classification classified the flight line images into 7 classes in order to correspond with the 7 classes that would be created with the supervised classification. In order for all pixels to be classified, no maximum standard deviation or minimum distance to the mean was specified. All ground plots were located on FL4 and FL7 and the class was recorded. A classification matrix was built for both FL4 and FL7 and it was determined that the ISODATA classification did not sufficiently separate the water repellency classes. Each unsupervised class that contained more than one of the ground truth points also had more than one class of water repellency values. Features such as water, vegetation, and granitic soil were the only distinguishable features with the ISODATA classification.

### *Supervised classification*

On FL4, the classification accuracy with 80 percent of the plots used as training pixels was very low. No more than one validation plot was correctly classified in to the correct water repellency class (no high water repellency plots were classified correctly). Part of the reason was the low number of validation pixels (4 or 5 per class). The probability of correctly classifying 4 pixels out of 4.5 million pixels per flight line was obviously low. Increasing the number of pixels used in validation would not necessarily increase the accuracy of the classification; it did however increase the probability of classification by increasing the chance. In addition, the spectral matching angle was increased from 0.1 to 0.2 radians in subsequent classifications. Increasing the angle decreased the exactness of spectral matching, however it allowed for more pixels to be classified. The unclassified area in this first classification was 50 percent, increasing the angle of difference lowered the unclassified area to 29 percent.

When 50 percent of the plots were used each as training pixels and validation pixels, the results were somewhat better. Similarly to the first classification, only one pixel in each of the water repellency classes was classified at the correct water repellency severity. Due to the high spatial variability of soil water repellency, adjacent pixels were examined for the presence of water repellency as well as water repellency severity (Figure 6). The pixel error from the geo-rectification is not known exactly, however there can safely assumed to be some degree of error. Therefore, examining surrounding pixels for water repellency is a reasonable approach. The predictability of the low water repellency

soils increased from 10 percent to 30 percent when the presence of adjacent water low repellent soils was considered in the accuracy assessment (Table 3). (Omission errors are reported in the table; accuracy is 100% minus the omission error.) The predictability of the moderate water repellent soils increased from 12 percent to 62 percent and the predictability of the high water repellent soils increased from 17 percent to 83 percent. The SAM classification does a better job of identifying the presence or absence of water repellent soils than predicting the water repellency severity. The overall accuracy of identifying water repellent soils (not water repellency severity) on FL4 considering the eight adjacent pixels to each study plot was almost 80 percent (Table 3). From the images, all three levels of soil water repellency occurred concurrently in fairly distinct regions (Figure 4). From an erosion potential standpoint, these would be the regions to focus on for erosion mitigation efforts. The identification of water repellent soils is likely more important than distinguishing between water repellency severity.

The remaining pixels on the image were classified into soil (12 percent), water (clouds on this flight line) (24 percent), and green (11 percent) and black (8 percent) canopy vegetation. The low and moderate water repellency plots were most often misclassified as soil, or else the low repellency plots would be classified as moderate repellency plots, and vice-versa. As previously stated, the spectral signatures of the low and moderate repellency plots were remarkably similar, nearly indistinguishable in the NIR and SWIR regions. Based on these initial results, a classification was run with the low and moderate plots combined into one single endmember. The results were better; six out of 19 plots were correctly classified into this new low/moderate class (previously two out of 19

with separate classes). The overall accuracy of determining the presence or absence of water repellent soils was slightly lower, however. The accuracy of identifying water repellent soils on surrounding pixels decreased to 74 percent.

On FL7, similar results were found as on FL4 using both sets of training pixels. No more than one pixel was correctly classified into any of the water repellency classes when 20 percent of the plots were used for validation. When 50 percent of the plots were reserved for validation, four out of 26 plots were correctly classified into water repellency classes. The low water repellency predictability increased from 17 percent to 67 percent when adjacent pixels were considered, the moderate water repellency predictability increased from 27 percent to 55 percent, and the high water repellency predictability increased from 0 percent to 45 percent (Table 4). (Again, omission errors are reported in the table; accuracy is 100% minus the omission error.) The overall accuracy of identification of the presence of water repellent soil for the FL7 study plots (examining surrounding pixels) was 81 percent. When the low and moderate water repellency classes were combined, five out of 17 plots were correctly classified into the combined class. The overall accuracy for the identification of water repellent soils on adjacent pixels dropped to 59 percent.

The remaining pixels on FL7 were classified as water (25 percent), soil (18 percent), green (7 percent) and black (6 percent) canopy vegetation. Again, the study plots were most often misclassified as soil or as a different water repellency class. The ground plots in this study are highly susceptible to misclassification. The ground cover varies greatly between water repellency plots, between different burn severities, and between

regions of the fire. The soil that was tested for water repellency was often surrounded by ash, charred organics, postfire needlecast, rock and green and black canopy. It was a combination of these organic and inorganic components that created the spectral signature associated with each of the water repellency classes. It was also the likely reason that many of the plots were misclassified (Tables 3 and 4) because of an overriding spectral signature different than the mean signatures of the three water repellency severities.

## **Conclusion**

The Hayman Fire was a large fire, more than half of which was initially classified as either a high or moderate severity burn. Typically, these are the areas that are thought to be at greatest risk for postfire erosion. Erosion mitigation is generally focused on high and moderate severity burn areas immediately after a fire in order to reduce the erosion potential during short duration, high intensity rain events. Without any further verification of these initial burn severity classes, this would mean a very large area would be treated for erosion control, regardless if the soil was actually likely to erode. *In situ* tests for soil water repellency provide reasonable estimates of soil infiltration potential, but only for a very small area at a time. Remote sensing of water repellent soils provides a method for a large area to be evaluated quickly, with fewer ground tests necessary.

The wavebands previously identified as useful for studying organic properties in soils were examined and it was found that there were no spectral features unique to the three different water repellency severity classes. Spectral features that may have existed were severely dampened by the widespread blackness within the burned areas. The spectral

signatures of the low, and high water repellency soils were significantly different over the entire range of wavebands ( $\alpha=0.05$ ), and moderate and high signatures were significantly different in the range 1500 to 1900 nm ( $\alpha=0.2$ ). These NIR bands were determined to be the most important for classifying water repellent soils remotely.

The supervised classification that was performed on the spectral data resulted in low accuracy for predicting the degree of water repellency severity of soils. However, the classification produced much better results for the prediction of the presence or absence of water repellent soils when neighboring pixels were examined. The accuracy was nearly 80 percent on both flight lines. These are reasonable accuracies when considering the scale of the fire and the erosion control that would typically be recommended based on these results. The different classes of soil water repellency occur together in well defined regions and would be easily identifiable for soil erosion mitigation. Approximately 16 percent of the area (1,700 ha) on both flight lines was classified as water repellent. When compared to the 32 percent of the area that was classified by the BAER map as high burn severity, 16 percent is a conservative estimate. It appears promising that remote sensing of water repellent soils will lead to a more accurate identification of erosion prone areas following forest fires.

### **Acknowledgements**

Special thanks to the field crews in Colorado during the summer of 2002 for their help collecting data. This research was supported by the USDA Forest Service Rocky Mountain Research Station and the USDA and USDI Forest Service Joint Fire Science

Program as well as the NSF Integrative Graduate Education and Research Training (IGERT) grant under NSF grant DGE-9972817 to the Center for Multiphase Environmental Research at Washington State University.

**Commercial Product Disclaimer**

The use of trade, firm, or corporation names in this publication is for the information and convenience of the reader. Such use does not constitute an official endorsement or approval by Washington State University or the United States Department of Agriculture of any product or service to the exclusion of others that may be suitable.

## References

- Almendros G, Gonzalez-Vila FJ, and Martin F. 1990. Fire-induced transformations of soil organic matter from an oak forest: An experimental approach to the effects of fire on humic substances. *Soil Science* **149(3)**: 158–168.
- Ben-Dor E, Banin A. 1995. Near-infrared analysis as a rapid method to simultaneously evaluate several soil properties. *Soil Science Society America Journal* **59**: 364–372.
- Chang D, Islam S. 2000. Estimation of soil physical properties using remote sensing and artificial neural network. *Remote Sensing of the Environment* **74**: 534–544.
- Clark RN. 1983. Spectral properties of mixtures of montmorillonite and dark carbon grains: Implications for remote sensing minerals containing chemically and physically adsorbed water. *Journal of Geophysical Research* **88(B12)**: 10,635–10,644.
- Clothier BE, Vogeler I, Magesan GN. 2000. The breakdown of water repellency and solute transport through a hydrophobic soil. *Journal of Hydrology* **231–232**: 255–264.
- Coleman TL, Montgomery OL. 1987. Soil moisture, organic matter, and iron content effect on the spectral characteristics of selected Vertisols and Alfisols in Alabama. *Photogrammetric Engineering and Remote Sensing* **53(12)**: 1659–1663.
- Colorado Climate Center. 2002.  
<http://climate.atmos.colostate.edu/dataaccess.shtml> [2003, January]
- DeBano LF. 2000a. The role of fire and soil heating on water repellency in wildland environments: a review. *Journal of Hydrology* **231–232**: 195–206.
- DeBano LF. 2000b. Water repellency in soils: a historical overview. *Journal of Hydrology* **231–232**: 4–32.
- DeBano LF, Savage SM, Hamilton DA. 1976. The transfer of heat and hydrophobic substances during burning. *Soil Science Society of America Journal* **40**: 779–782.
- Decagon Devices Inc. 1998.  
<http://www.decagon.com/instruments/infilt.html> [2003, June]
- Dekker LW, Ritsema CJ. 1994. How water moves in a water repellent sandy soil 1. Potential and actual water repellency. *Water Resources Research* **30**: 2507–2517.

- ENVI version 3.4. 2000. The Environment for Visualizing Images, Version 3.4, Research Systems, Inc., Boulder, CO.  
<http://www.rsinc.com/envi> [2003, October]
- Fidencio PH, Poppi RJ, de Andrade JC. 2002. Determination of organic matter in soils using radial basis function networks and near infrared spectroscopy. *Analytica Chimica Acta* **453**: 125–134.
- Giovannini G, Lucchesi S. 1997. Modifications in soil physico-chemical parameters by experimental fires at different intensities. *Soil Science* **1627**: 479–486.
- Giovannini G, Lucchesi S. 1984. Differential thermal analysis and infrared investigations on soil hydrophobic substances. *Soil Science* **1376**: 457–463.
- Graham RT, (tech. ed.). 2003. *Hayman Fire Case Study*. Gen. Tech. Rep. RMRS-GTR-114. USDA Forest Service, Rocky Mountain Research Station, Ogden, UT; 396p.
- Henderson TL, Baumgardner MF, Franzmeier DP, Stott DE, Coster DC. 1992. High dimensional reflectance analysis of soil organic matter. *Soil Science Society America Journal* **56**: 865–872.
- Henderson TL, Szilagyi A, Baumgardner MF, Chen CT, Landgrebe DA. 1989. Spectral band selection for classification of soil organic matter content. *Soil Science Society America Journal* **53**: 1778–1784.
- Huffman EL, MacDonald LH, Stednick JH. 2001. Strength and persistence of fire-induced soil hydrophobicity under ponderosa and lodgepole pine, Colorado Front Range. *Hydrological Processes* **15**: 2877–2892.
- Hummel JW, Sudduth KA, Hollinger SE. 2001. Soil moisture and organic matter prediction of surface and subsurface soils using an NIR soil sensor. *Computers and Electronics in Agriculture* **32**: 149–165.
- Jackson TJ, LeVine DM. 1996. Mapping surface soil moisture using an aircraft-based passive microwave instrument: algorithm and example. *Journal of Hydrology* **184**: 85–99.
- Jackson TJ, LeVine DM, Swift CT, Schmugge TJ, Schiebe FR. 1995. Large area mapping of soil moisture using the ESTAR passive microwave radiometer in Washita '92. *Remote Sensing of the Environment* **53**: 27–37.
- Jensen JR. 1996. *Introductory Digital Image Processing*. Prentice Hall, New Jersey; 318p.

- Letey J. 2001. Causes and consequences of fire-induced soil water repellency. *Hydrological Processes* **15**: 2867–2875.
- Letey J, Carrillo MLK, Pang XP. 2000. Approaches to characterize the degree of water repellency. *Journal of Hydrology* **231–232**: 61–65.
- Lewis SA, Wu JQ, Robichaud PR. 2003. Determining fire-induced soil water repellency using water drop penetration time and mini-disk infiltrometer tests. *Hydrological Processes*, in review.
- Nishita H., Haug RM. 1972. Some physical and chemical characteristics of heated soils. *Soil Science* **113**: 422–430.
- Palacios-Orueta A, Ustin SL. 1998. Remote sensing of soil properties in the Santa Monica Mountains I. Spectral Analysis. *Remote Sensing of the Environment* **65**: 170–183.
- Parsons A. 2003. Burned area emergency rehabilitation (BAER) soil burn severity definitions and mapping guidelines. Unpublished report. USDA Forest Service Remote Sensing Application Center, Salt Lake City, UT.
- Patterson MW, Yool SR. 1998. Mapping fire-induced vegetation mortality using Landsat Thematic Mapper data: A comparison of linear transformation techniques. *Remote Sensing of the Environment* **65**: 132–142.
- Richards JA, Jia, X. 1999. *Remote Sensing Digital Image Analysis: an introduction*. Springer, New York; 363p.
- Robichaud PR. 2000. Fire effects on infiltration rates after prescribed fire in Northern Rocky Mountain forests, USA. *Journal of Hydrology* **231–232**: 220–229.
- Robichaud PR, Hungerford RD. 2000. Water repellency by laboratory burning of four northern Rocky Mountain forest soils. *Journal of Hydrology* **231–232**: 207–219.
- SAS Institute Inc. 1999a. *SAS/STAT<sup>®</sup> User's Guide, Volume 1, Version 8.2*. Statistical Analysis Systems (SAS) Institute Inc., Cary, NC.
- Savage SM, Osborn J, Letey J, Heaton C. 1972. Substances contributing to fire-induced water repellency in soils. *Soil Science Society of America Proceedings* **36**: 674–678.
- Schmid EM, Skjemstad JO, Glaser B, Knicker H, Kogel-Knabner I. 2001. Detection of charred organic matter in soils from a Neolithic settlement in Southern Bavaria, Germany. *Geoderma* **1788**: 1–23.

- Smith RT, Atkinson K. 1975. *Techniques in Pedology: a handbook for environmental and resource studies*. Elek, London; 213 p.
- Sudduth KA, Hummel JW. 1991. Evaluation of reflectance methods for soil organic matter sensing. *Transactions of the ASAE* **34(4)**: 1900–1909.
- University of Colorado. 2003. Cooperative Institute for Research in Environmental Sciences, ATREM frequently asked questions.  
<http://cires.colorado.edu/cses/atrem.html> [2003, October]
- USDA Forest Service. 2002. Burned Area Report, Hayman Fire, Pike and San Isabelle National Forests.  
[http://wildfiresw.nwcg.gov/colorado/baer/hayman\\_fire\\_BAER\\_final.htm](http://wildfiresw.nwcg.gov/colorado/baer/hayman_fire_BAER_final.htm) [2003, April]
- USDA Forest Service Remote Sensing Applications Center. 2003. Burned Area Emergency Rehabilitation (BAER) Imagery Support.  
<http://www.fs.fed.us/eng/rsac/baer/> [2003, October]
- Zhang R. 1997. Determination of soil sorptivity and hydraulic conductivity from the disk infiltrometer. *Soil Science Society America Journal* **61**: 1024–1030.

Table 1. Correlation between WDPT test and ranges of wavebands. Tukey test of means between high and low water repellency and between high and moderate water repellency over different waveband ranges. Means are either significantly different (S) or not significantly different (NS). Significant  $p$ -values are in parenthesis. Note  $\alpha$  values are different between the two Tukey tests.

Waveband Range (nm)	ANOVA			
	Correlation		Tukey Means	
	WDPT	$p$ -val ( $\alpha=0.05$ )	High vs. Low ( $\alpha=0.05$ )	High vs. Mod ( $\alpha=0.2$ )
432–707	-0.26	0.0006	S (0.023)	NS
722–992	-0.25	0.0008	S (0.025)	NS
1007–1496	-0.28	0.0001	S (0.012)	NS
1510–1791	-0.29	<0.0001	S (0.009)	S (0.05)
2056–2512	-0.26	0.0003	S (0.025)	NS

Table 2. Soil characteristics and ground cover characteristics by flight line and water repellency (WR) classification.

<b>Flight Line &amp; WRClass</b>	<b>Soil Characteristics</b>			<b>Ground Cover Characteristics</b>				
	OM (%)	WDPT (s)	Infil. (ml/min)	Ash (%)	Soil (%)	Charred Soil (% of Soil)	Litter (%)	Charred Litter (% of Litter)
FL4 Low	4.4	25	7.6	8	70	27	17	68
FL4 Mod	6.2	116	2.9	17	57	32	21	60
FL4 High	9.7	225	2.9	26	39	56	30	39
FL7 Low	4.7	34	6.1	22	53	16	18	100
FL7 Mod	5.0	133	3.9	20	42	18	34	62
FL7 High	5.9	253	1.9	27	23	32	41	48

Table 3. Classification matrix of FL4 with half of the pixels used as validation pixels. Omission error 1 is the percent of validation pixels that were not classified at the correct water repellency severity. Omission error 2 is the percent of validation pixels that were not classified correctly or adjacent to a pixel of the correct water repellency severity. Omission error 3 is the percent of validation pixels that were not classified correctly or adjacent to any pixel classified as water repellent.

<b>Classification</b>	<b>Validation Pixels</b>			<b>Total</b>
	<b>Low WR <i>n</i>=10</b>	<b>Moderate WR <i>n</i>=8</b>	<b>High WR <i>n</i>=6</b>	
Low WR	1	2	0	3
Moderate WR	3	1	1	5
High WR	0	1	1	2
Soil or Vegetation	3	4	2	9
Unclassified	3	0	2	5
Total	10	8	6	24
<b>Omission Error 1 (%)</b>	<b>90</b>	<b>88</b>	<b>83</b>	<b>58</b>
Adjacent to same severity WR pixel	3	5	5	13
<b>Omission Error 2 (%)</b>	<b>70</b>	<b>38</b>	<b>17</b>	<b>46</b>
Adjacent to any severity WR pixel	7	7	5	19
<b>Omission Error 3 (%)</b>	<b>30</b>	<b>13</b>	<b>17</b>	<b>21</b>

Table 4. Classification matrix for FL7 with half of the pixels used as validation pixels. Omission error 1 is the percent of validation pixels that were not classified at the correct water repellency severity. Omission error 2 is the percent of validation pixels that were not classified correctly or adjacent to a pixel of the correct water repellency severity. Omission error 3 is the percent of validation pixels that were not classified correctly or adjacent to any pixel classified as water repellent.

<b>Classification</b>	<b>Validation Pixels</b>			<b>Total</b>
	<b>Low WR <i>n</i>=6</b>	<b>Moderate WR <i>n</i>=11</b>	<b>High WR <i>n</i>=9</b>	
Low WR	1	1	3	5
Moderate WR	1	3	0	4
High WR	0	1	0	1
Soil or Vegetation	1	5	3	9
Unclassified	3	1	3	7
Total	6	11	9	26
<b>Omission Error 1 (%)</b>	<b>83</b>	<b>73</b>	<b>100</b>	<b>62</b>
Adjacent to same severity WR pixel	4	6	4	14
<b>Omission Error 2 (%)</b>	<b>33</b>	<b>45</b>	<b>55</b>	<b>46</b>
Adjacent to any severity WR pixel	5	8	8	21
<b>Omission Error 3 (%)</b>	<b>17</b>	<b>27</b>	<b>11</b>	<b>19</b>

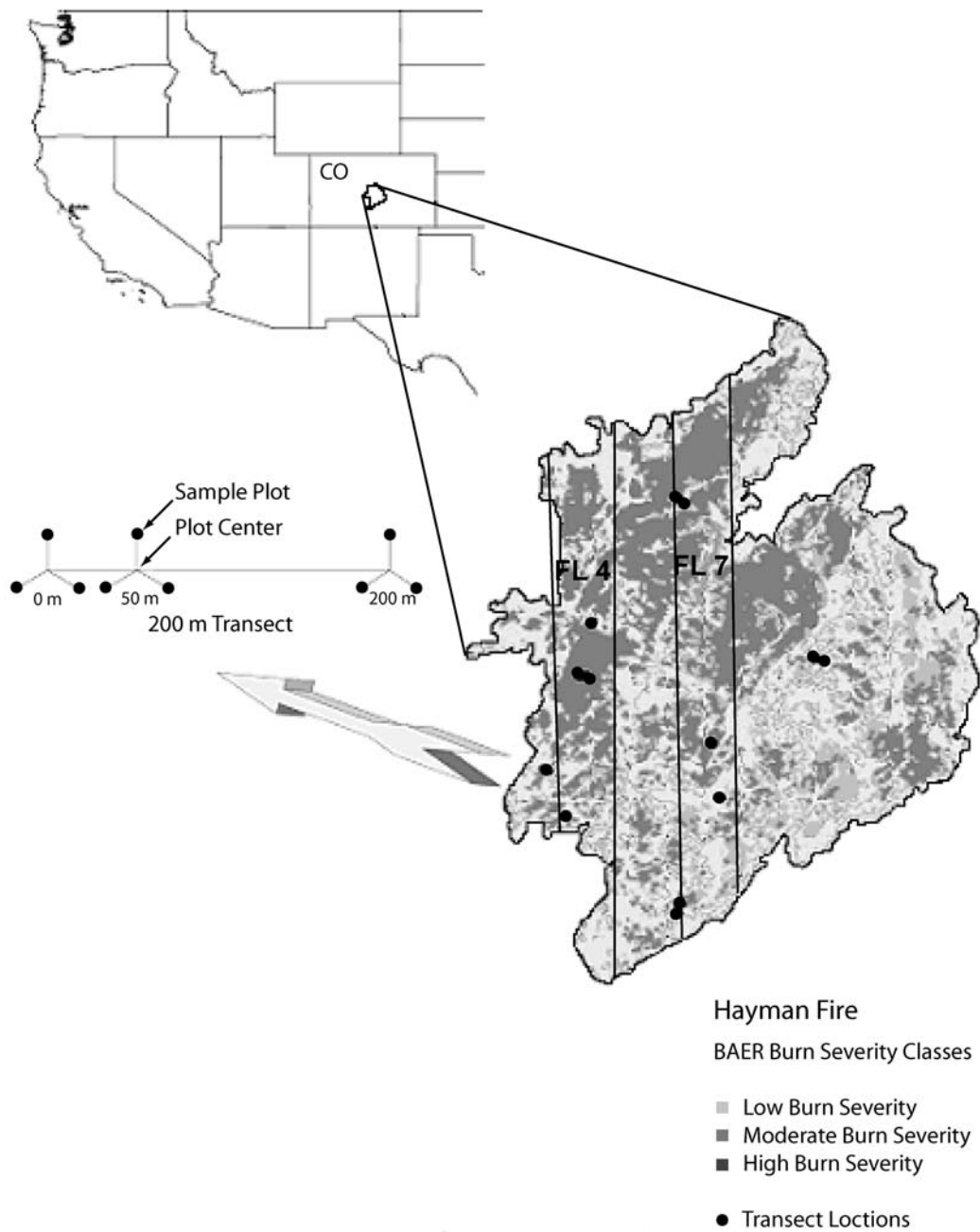


Figure 1. Hayman Fire location, transect locations within fire, and transect layout. Flight lines 4 (FL4) and 7 (FL7) are shown on the BAER burn severity map.

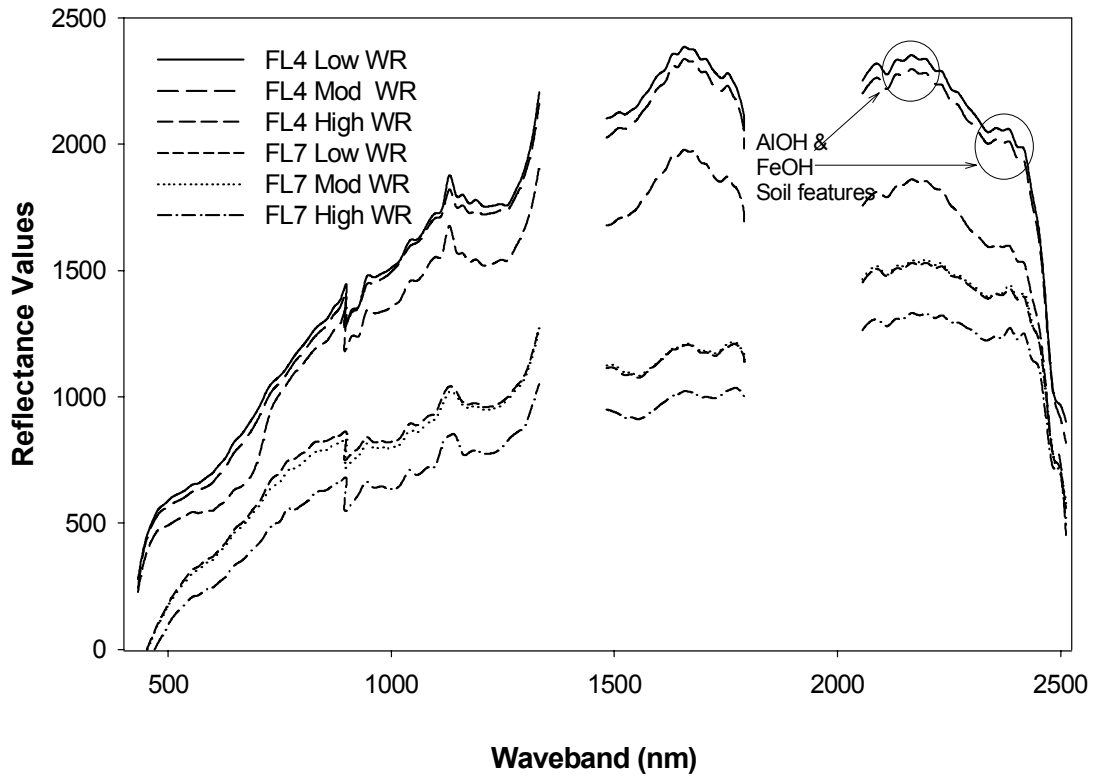


Figure 2. Mean reflectance values for the three water repellency endmembers for both flight lines across all measured wavebands. Visible soil mineral features (Aluminum Hydroxide and Iron Hydroxide) are circled on FL4. Gaps at 1400 and 1900 nm are atmospheric water absorption bands that were excluded due to the noise in these bands.

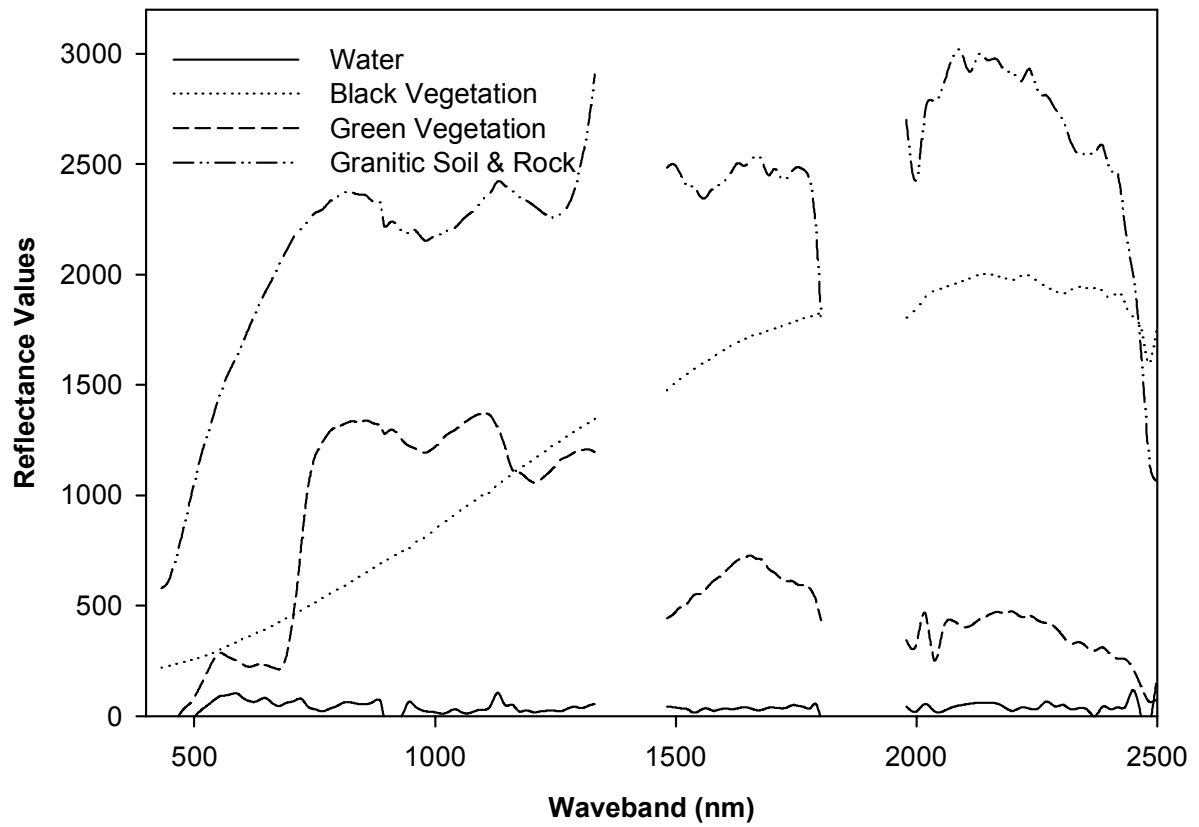


Figure 3. Granitic soil and rock, water, green and black vegetation endmembers plotted across all measured wavebands. Gaps at 1400 and 1900 nm are atmospheric water absorption bands that were excluded due to the noise in these bands.

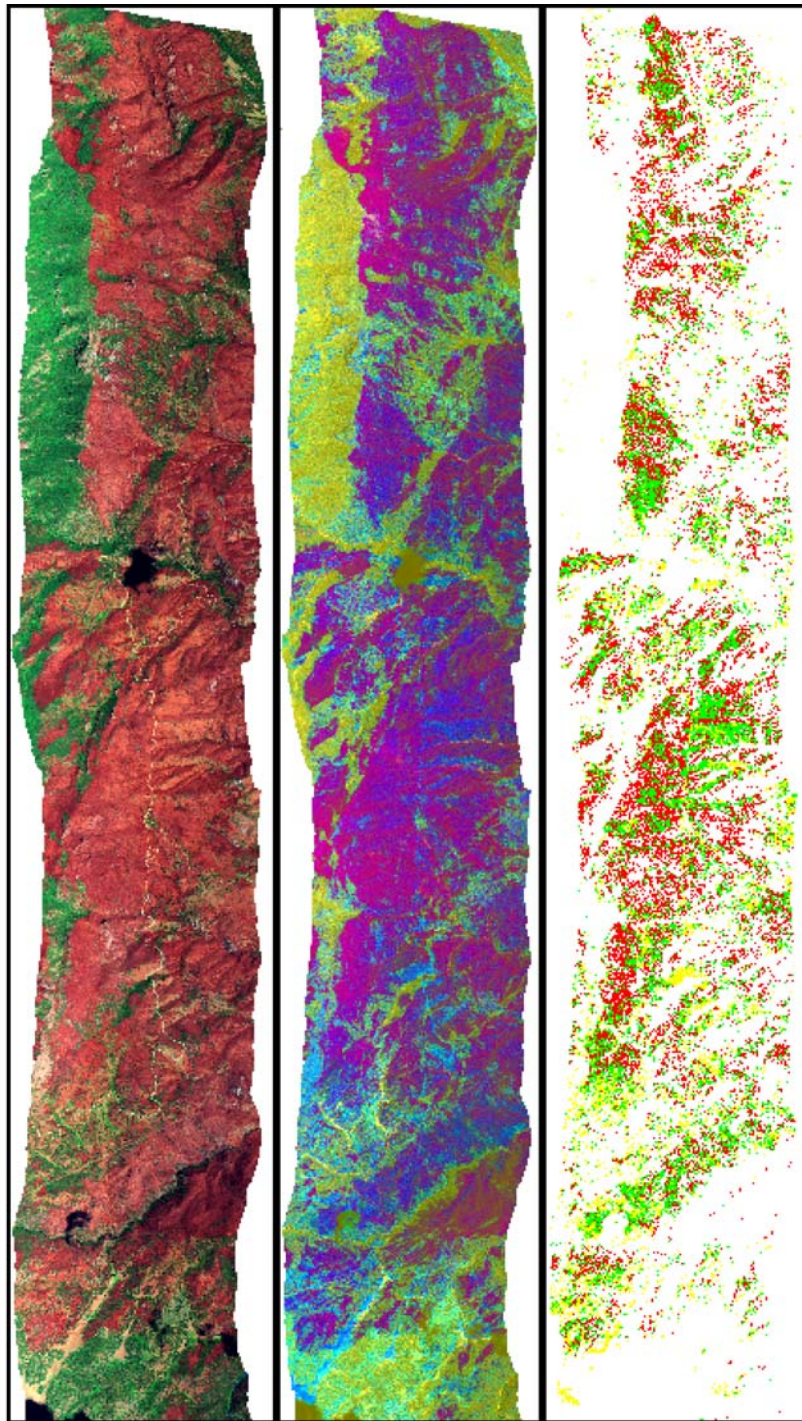


Figure 4. Flight Line 4 images. Left image is Red, Green, Blue (bands 118, 36,9); red areas are burned soil and vegetation, green highlights live vegetation, and light colored areas are granitic soil and rocks. Middle image is PC bands (3,2,1); red representing deep burn, green representing vegetation, and blue representing soils. Right image is SAM classified image with three water repellency classes:

■ Low WR   
 ■ Moderate WR   
 ■ High WR

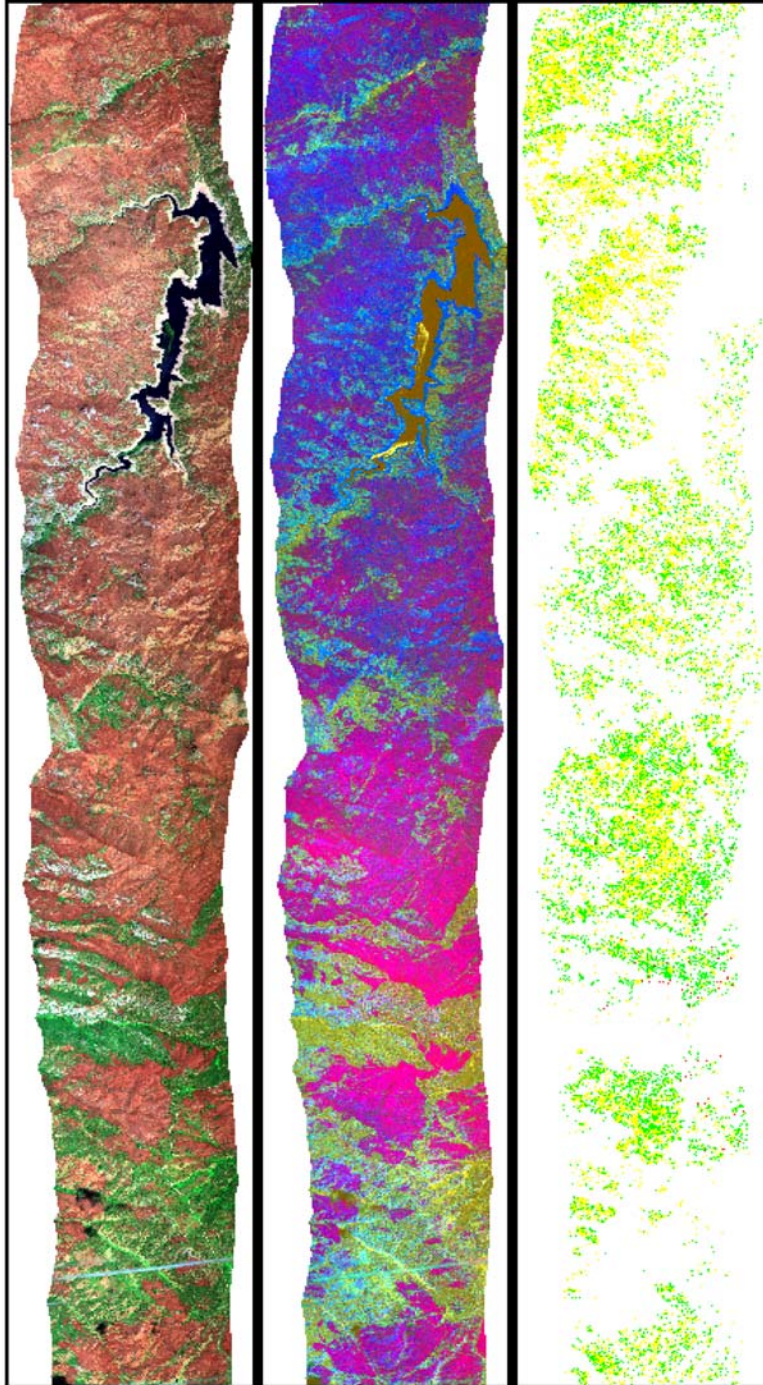


Figure 5. Flight Line 7 images. Left image is Red, Green, Blue (118, 36,9); red areas represent burned soil and vegetation, green highlights live vegetation, and light colored areas are granitic soil and rocks. Middle image is PC bands (3,2,1); red representing deep burn, green representing vegetation, and blue representing soils. Right image is SAM classified image with three water repellency classes:

■ Low WR   
 ■ Moderate WR   
 ■ High WR

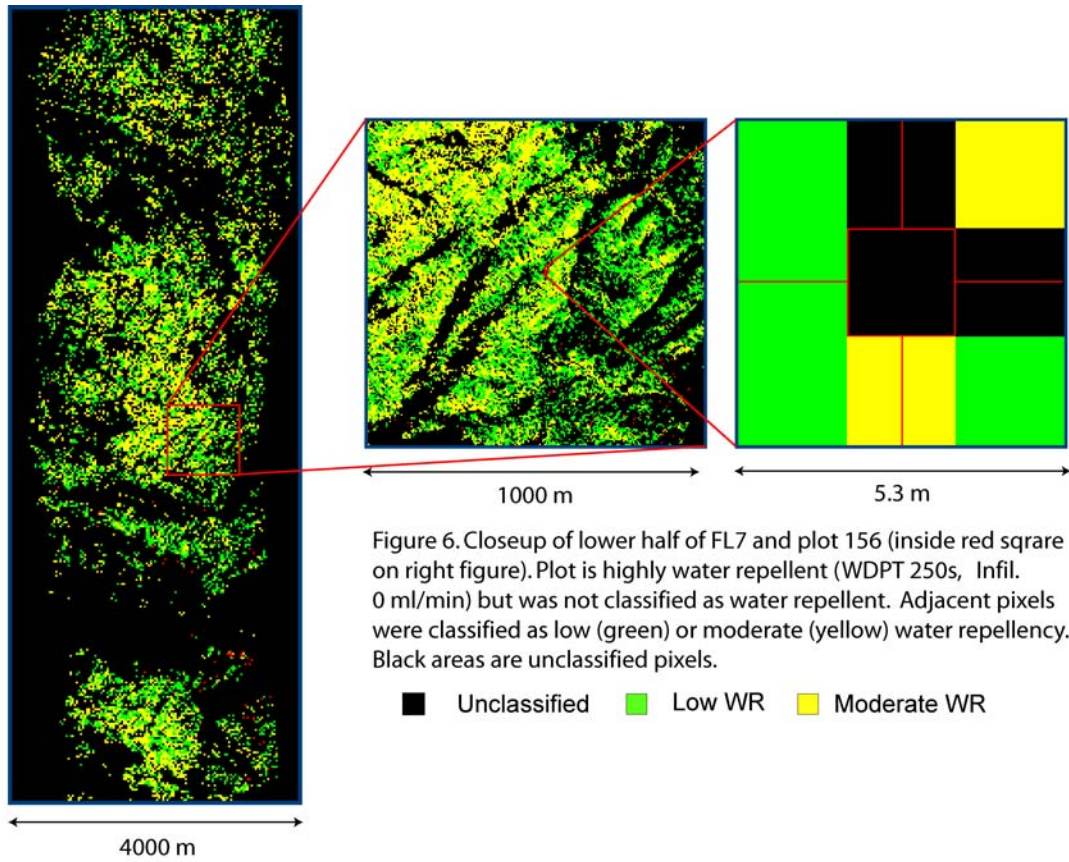


Figure 6. Closeup of lower half of FL7 and plot 156 (inside red square on right figure). Plot is highly water repellent (WDPT 250s, Infil. 0 ml/min) but was not classified as water repellent. Adjacent pixels were classified as low (green) or moderate (yellow) water repellency. Black areas are unclassified pixels.

## CHAPTER FOUR

### CONCLUSION

After extensive ground sampling, as well as analyzing two remotely sensed images, several conclusions can be made regarding the Hayman Fire. Nearly 60,000 ha burned, and over half of the area was initially classified as a moderate or high severity burn. It is on these severely burned areas that erosion mitigation is typically focused. Part of the goal of this study was to validate or invalidate traditional methods for estimating soil burn severity and the subsequent erosion potential. Two new technologies were applied and the results were evaluated and compared to the traditional methods. The new tests were for on-site and for remote determination of soil erosion prediction potential and the results of both seem promising.

Based on the burn severity map created by the BAER team, study sites were picked in each of three burn severity classes: low, moderate and high. At these sites, both organic and inorganic ground cover components were studied in order to evaluate the degree of severity of burn. Water repellency tests were performed to assess the likelihood of postfire soil erosion. Based on the soil and vegetation indices measured in the field, the burn severity classes that were initially assigned by the BAER teams seem reasonable. With regard to the water repellency tests, many of the areas that were classified as high burn severity did not have highly water repellent soils, as expected. The moderate burn sites had more consistent and pronounced soil water repellency. Some of the high burn severity areas burned very quickly; the residence time of the fire was not long and soil heating did

not go deep or to a high temperature. Overall, some of the areas that were classified as high severity burn were probably over-classified; they should have been placed into the moderate category.

About half of the variables measured in the burn area were significant for determining burn severity. Many of these variables also had a significant relationship with soil water repellency. By measuring key soil and vegetation factors, along with the WDPT or infiltrometer test, site burn severity and water repellency can be adequately determined. Both WDPT and infiltrometer tests indicated similar water repellency results within each burn severity class. The WDPT and infiltrometer values were strongly correlated at each individual burn severity class as well as overall. The two tests were shown to be compatible and should be used to complement each other. After the infiltrometer has been tested more extensively, it may replace the WDPT for *in situ* determination of soil water repellency. The subjectivity of the WDPT has been removed with the infiltrometer, and the test time is cut in half. If subsequent measurements are made with the infiltrometer, the soil's hydraulic conductivity can be determined as well. The additional quantitative information the infiltrometer can provide should prove to be more useful than the WDPT.

Both infiltrometer and WDPT tests for soil water repellency provide reasonable estimates of soil infiltration potential, but only for a very small area at a time. The need to assess a large area quickly after a fire for erosion mitigation leads to the need for remote sensing technology. Remote sensing of soil burn severity and water repellent soils provides a means for a large area to be evaluated quickly, with fewer ground tests necessary to validate the erosion potential.

Upon analyzing the wavebands previously identified as useful for studying organic properties in soils were examined and it was found that there were no spectral features unique to the three different water repellency severity classes. Spectral features that may have existed were severely dampened by the widespread blackness within the burned areas. The spectral signatures of the low, and high water repellency soils were significantly different over the entire range of wavebands ( $\alpha=0.05$ ), and moderate and high signatures were significantly different in the range 1500 to 1900 nm ( $\alpha=0.2$ ). These NIR bands were determined to be the most important for studying water repellent soils remotely.

The supervised classification that was performed on the spectral data resulted in low accuracy for predicting water repellency severity of soils. However, the classification produced much better results for the prediction of the presence or absence of water repellent soils when neighboring pixels were examined. The accuracy was at least 80 percent on both flight lines. These are reasonable accuracies when considering the scale of the fire and the erosion control that would typically be recommended based on this type of study. The different classes of soil water repellency occur together in well defined regions and would be easily identifiable for soil erosion mitigation. Approximately 16 percent of the area (1,700 ha) on both flight lines was classified as water repellent. When compared to the 32 percent that was classified by the BAER map as high burn severity, 16 percent is a conservative estimate. It is also interesting to note that the regions that were identified as high burn severity are not exactly the areas that tested positive for water repellency, or were predicted water repellent by the image classification. As stated earlier, some of the high burn severity areas were misclassified by the initial burn severity map. This is more

evidence that previous methods of postfire burn and erosion mapping need to be re-evaluated. It appears promising that remote sensing of water repellent soils will lead to a more accurate identification of erosion prone areas following forest fires. This study is a first attempt to specifically target the measurement of water repellent soils remotely. For a first effort, the results seem reasonable, with a realistic percentage of the fire area being classified as water repellent.

APPENDIX A  
FIELD DATA FORMS  
AND INSTRUCTIONS

Water Repellency Data Sheet																
Fire					Date				Crew				Time of day			
Burn Classification					Transect				Plot				Subplot	0 (N)	120	240
Soil sample taken/labeled		Y	N		GPS		Y	N		Picture number on camera						
	Position along transect															
Infiltration Depth	0 cm	5 cm	10 cm	15 cm	20 cm	25 cm	30 cm	35 cm	40 cm	45 cm	50 cm					
0 cm																
1 cm																
2 cm																
3 cm																
4 cm																
5 cm																
Infiltration Time																
<i>Perform infiltrometer tests at these approximate positions along the corresponding Water Drop transect</i>																
	Infiltrometer Test 1			Infiltrometer Test 2			Infiltrometer Test 3			Infiltrometer Test 4						
Initial water level (ml)																
Time to start of Infiltration (s)																
Final water level (ml)																
Volume infiltrated (ml)																

Figure Appendix A1. Water repellency data field form. Eleven water drop tests and four infiltrometer tests were performed at each subplot.

## **Instructions for using Water Repellency Data Sheet:**

- ✓ Plot ID includes specific transect number, plot ID, subplot ID [0(N), 120, 240]
- ✓ Burn Classification: low, moderate, high
- ✓ Collect an undisturbed surface soil sample in the soil can, seal with tape and label with a permanent marker
- ✓ Many plots will be identified by a GPS, note sample ID if applicable

### **Water Drop Penetration Time (WDPT) test**

Water drops will be placed at 5 cm spacing across a 0.5 m plot. There is room on the data sheet for 11 drops. The first drops are placed on the surface (mineral soil). Gently remove ash and litter layer if necessary. If the water drops do not infiltrate within 5 seconds, the soil is considered water repellent. Allow the water drops to remain on the surface until infiltration occurs. Note the time to infiltration. If the water drops still have not infiltrated after 5 minutes, note this as well and move on.

For water drops that infiltrate in less than 5 seconds, dig to a depth of 1cm and repeat the process above. If necessary, continue the process up to a depth of 2 cm, in 1 cm increments. Be sure and note the time and depth at which the water drop remains on the soil surface for longer than 5 seconds.

### **Infiltrometer**

Fill the infiltrometer with water (it will not leak once it is sealed). Gently level a spot in the center of the plot on the soil surface (not ash surface). Note initial volume of water in the infiltrometer and place the filled infiltrometer on the soil. Hold in place level and firmly. Note the time (seconds) to the first air bubble; this indicates the start of infiltration. Measure the volume of water that infiltrates in 1 minute.

### Burn Severity Form

Date \_\_\_ State **CO** Fire or watershed name **Hayman Fire** Transect \_\_\_ Plot \_\_\_ Subplot \_\_\_

Aspect \_\_\_ Slope % \_\_\_ Slope position \_\_\_ GPS coord. (lat, long) \_\_\_\_\_

Crew \_\_\_\_\_ Page \_\_\_\_\_

Strata	Total Cover	Unburned	Lt. Char	Mod. Char	Deep Char	Comment						
<b>Ground surface – 1/300<sup>th</sup> acre plot (4 m diameter)</b>												
Ash		Unrecognizable as plant material										
Water												
new litter		Type (fir or pine, shrub)										
Litter												
Humus												
Mineral soil												
Rock (diameter < than 1")												
BCC												
CWD < 3"												
CWD >= 3"												
Stump human or natural												
New litter thick ___ mm Litter thick ___ mm Humus thick ___ mm												
<i>Comments on rills and soil erosion:</i>												
<b>Grass, Forbs, low shrubs (&lt; 1.5 ft or 0-1/4 in basal dia.) - 1/300<sup>th</sup> acre plot (4 m diameter)</b>						Dominant Species						
Grass												
Forbs												
new tree seedlings (#)												
Low shrubs(#)												
<b>Medium (1.5 - 6 ft or 1/4-1 in basal dia) and tall shrubs (&gt; 6 ft or &gt;1 in), and saplings (upto 4.9 in) – 1/300<sup>th</sup> acre plot (4 m diameter)</b>												
Medium shrubs(#)												
Tall shrubs(#)												
Saplings(#)	#	#	#	#	#							
<b>Trees (&gt; 4.9 in dbh) trees - 1/24<sup>th</sup> acre plot (20 m diameter)</b>												
				If Crown Present			Snag		Bole Scorch ht			
# Tree	Sp	Ht	DBH & Basal dia.	CR	% gm	% brn	% blk	creat	Cond	low/dir	high/dir	Comment
Variable Plot: BA _____ = for trees greater than 18" outside the 1/24th acre fixed plot												
<i>Comment on Trees greater than 4.9 and other general comments:</i>												
* = mistle toe												
Stem % black												

Figure Appendix A2. Burn severity data field form. Organic and inorganic ground cover components of subplots are recorded along with the percent char of each.

## Explanation of terms and Instructions for Burn Severity Data Sheet

### **STRATUM: GROUND SURFACE**

Total cover (%) for each soil component on a 1/300<sup>th</sup> acre plot

**Ash:** Loose burnt unrecognizable material

**Water:** Visible surface water not just moisture

**New litter:** litter fallen onto the ground surface since fire  
Litter type

**Previous Litter:** loose undecomposed material

Percent of total cover that is:

Unburned: no sign of charcoal

Light Char: blackened but definable as plant parts

**Previous Humus:** decomposed organic layer below litter

Unburned: no sign of charcoal

Light Char: blackened but can find

### **Surface Mineral soil**

Unburned: no sign of charcoal

Light char: blackened

Moderate char: ash colored (grey)

Deep char: orange

**BCR:** brown or white cubical rotten wood

Unburned: no sign of charcoal

Light char: burned on surface

Moderate char: burned but still present

Deep char: imprint on soil surface

**CWD < 3":** woody debris less than 3" in diameter (sticks)

Unburned: no sign of charcoal

Light char: burned on surface but still see unburned areas on sticks

Moderate char: all sticks are charred (all black)

**CWD > 3":** woody debris greater than 3" (small to large logs)

Unburned: no sign of charcoal

Light char: blackened or scorched but still see unburned areas

Moderate char: all blackened and charring goes into the wood

Deep char: only large logs are present and are deeply charred

**Stump:** sound human created stumps (post-harvest)

Unburned: no sign of charcoal

Light char: stumps intact but blackened

Moderate char: burned deep enough to form charcoal

Deep char: stump gone, hole in ground

New litter, previous litter, and previous humus depth: take at 4 cardinal directions at center of 6.8' pole in mm.

**STRATUM: GRASS, FORBS, SMALL SHRUBS (< 1.5 ft), SEEDLINGS (< 1 in dbh)**

Total cover (%) for each component on a 1/300th acre plot

Proportion of total cover that is

Unburned should be the same)

Light char: blackened soil with shrubs or forbs present; small seedlings not yet established

**STRATUM: MEDIUM (1.5-6 ft) AND TALL SHRUBS (> 6 ft) AND SAPLINGS (1-4.9 dbh in)**

Total cover (%) for each component on a 1/24th acre plot

Proportion of total cover that is

Unburned

Light char: part of the shrub is blackened (usually at base) and stems still in tact

Moderate char: stub of shrub exists

Deep char: holes left from shrubs

**Saplings**

Unburned

Light char: blackened but some needles (live or dead) exist on trees

Moderate char: dead trees with bare stems

Deep Char: holes left from stumps

**STRATUM: TREES**

# Tree: number of intermediate trees that express similar fire severity

Species: PP; DF, ES, AF, LP

Ht: estimated height of tree

CR = crown ratio

Unburned - no sign of burned area

Proportion of crown ratio that is:

% green: percent of crown with green needles

% brown: percent crown with brown needles

% black: no needles

Snag:

Creat = creation source

1 trees dead due to fire

2 snags prior to fire

Cond = condition of snag

3 mostly intact

4 loose bark

5 bark fallen off or beetle evidence

6 top broken (precedence over 3,4,5)

7 decomposed standing

8 snag fallen over (preced.over all codes)

Bole scorch height

Low: low char height and direction it faces

High: high char height and direction it faces

% **blackened**: percent stem blackened at base of tree above forest floor surface

APPENDIX B

WATER REPELLENCY DATA

Number	Plot	Severity	WDPT (s)	Infil (ml/min)
1	L7-1-0m-340	L	214	1.33
2	L7-1-0m-120	L	111	1.75
3	L7-1-0m-240	L	86	2.33
4	L7-50m-0	L	63	6.67
5	L7-50m-120	L	54	5.75
6	L7-50m-240	L	160	0.75
7	L7-1-200m-0	L	123	5.75
8	L7-1-200m-120	L	197	10.50
9	L7-1-200m-240	L	0	7.75
10	L7-2-0m-0	L	117	3.50
11	L7-2-0m-120	L	181	0.00
12	L7-2-0m-240	L	0	8.75
13	L7-2-150m-0	L	129	2.50
14	L7-2-150m-120	L	100	5.25
15	L7-2-150m-240	L	161	7.75
16	L7-2-200m-0	L	245	1.25
17	L7-2-200m-120	L	45	5.75
18	L7-2-200m-240	L	167	7.50
19	L8-0m0	L	4	8.13
20	L8-0m120	L	5	6.38
21	L8-0m240	L	262	0.38
22	L8-150m0	L	51	9.38
23	L8-150m120	L	0	11.13
24	L8-150m240	L	87	3.25
25	L8-200m0	L	35	3.38
26	L8-200m120	L	3	8.75
27	L8-200m240	L	15	6.25
28	L8-2-0m0	L	25	4.13
29	L8-2-0m120	L	263	3.25
30	L8-2-0m240	L	140	7.63
31	L8-2-50m0	L	106	3.50
32	L8-2-50m120	L	9	5.38
33	L8-2-50m240	L	0	10.25
34	L9-1-0m0	L	0	8.00
35	L9-1-0m120	L	262	0.50
36	L9-10m240	L	74	4.75
37	L9-1-50m0	L	48	4.75
38	L9-150m120	L	128	4.00
39	L9-1-50m240	L	134	3.00
40	L9-1200m0	L	234	1.25
41	L9-1-200m120	L	214	2.75
42	L9-1-200m240	L	16	4.50
43	L9-2-50m-0	L	82	1.00
44	L9-2-50m120	L	35	5.25
45	L9-2-50m-240	L	123	2.25
46	L9-2-200m-0	L	298	0.00
47	L9-2-200m-120	L	244	7.00
48	L9-2-200m-240	L	104	1.75
49	L10-1-0m-0	L	185	9.00
50	L10-1-0m-120	L	168	2.50
51	L10-1-0m-240	L	53	2.25
52	L10-1-50m-0	L	79	4.75
53	L10-1-50m-120	L	11	8.50
54	L10-1-50m-240	L	55	2.25
55	L10-1-200m-0	L	247	3.25
56	L10-1-200m-120	L	188	10.50
57	L10-1-200m-240	L	242	0.25
58	L10-2-80m-0	L	103	2.75
59	L10-2-80m-120	L	35	11.25
60	L10-2-80m-240	L	28	7.75
61	L10-2-200m-0	L	273	0.00
62	L10-2-200m-120	L	99	8.00
63	L10-2-200m-240	L	183	2.25

Figure Appendix B1. Low burn severity WDPT and Infiltrometer values.

Number	Plot	Severity	WDPT (s)	Infil (ml/min)
64	M1-0m0	M	200	1.8
65	M1-0m120	M	183	0.6
66	M1-0m240	M	124	8.9
67	M1-50m0	M	218	1.3
68	M1-50m120	M	300	0.1
69	M1-50m240	M	282	1.5
70	M1-200m0	M	224	1.0
71	M1-200m240(1)	M	120	6.8
72	M1-200m240(2)	M	197	3.8
73	M2-0m0	M	123	4.1
74	M2-0m120	M	283	0.8
76	M2-50m0	M	160	8.0
77	M2-50m120	M	173	1.8
78	M2-50m240	M	137	2.1
79	M2-200m0	M	173	3.3
80	M2-200m120	M	30	2.8
81	M2-200m240	M	178	1.3
82	M3-0m0	M	84	5.0
83	M3-0m120	M	9	6.9
84	M3-0m240	M	63	8.9
85	M3-50m0	M	253	0.9
86	M3-50m120	M	16	13.6
87	M3-50m-240	M	179	0.9
88	M3-200m0	M	0	10.4
89	M3-200m120	M	28	7.0
90	M3-200m240	M	137	3.3
91	M4-0m120(1)	M	11	6.9
92	M4-0m120(2)	M	52	3.6
93	M4-0m-240	M	80	2.9
94	M4-50m0	M	21	4.5
95	M4-50m120	M	274	0.2
96	M4-50m-240	M	99	0.9
97	M4-200m0	M	255	1.9
98	M4-200m120	M	171	3.4
99	M4-200m240	M	46	4.4
100	M4-2-0m0	M	300	0.3
101	M4-2-0m120	M	300	0.0
102	M4-2-0m240	M	248	0.0
103	M4-2-50m0	M	31	6.9
104	M4-2-50m120	M	248	1.4
105	M4-2-50m240	M	165	3.0
107	L6-1-0m-0	M	52	1.0
108	L6-1-0m-120	M	274	3.8
109	L6-1-0m-240	M	230	5.3
110	L6-1-50m-0	M	281	3.3
111	L6-1-50m-120	M	90	3.3
112	L6-1-50m-240	M	273	0.8
113	L6-1-200m-0	M	300	0.3
114	L6-1-200m-120	M	105	3.8
115	L6-1-200m-240	M	300	0.2
116	L6-2-0m-0	M	214	4.3
117	L6-2-0m-120	M	206	0.0
118	L6-2-0m-240	M	50	3.3
119	L6-2-50m-0	M	248	4.8
120	L6-2-50m-120	M	163	0.3
121	L6-2-50m-240	M	140	9.0
122	L6-2-200m-0	M	57	6.0
123	L6-2-200-120	M	272	3.4
124	L6-2-200m-240	M	65	7.1

Figure Appendix B2. Moderate burn severity WDPT and Infiltrometer values.

Number	Plot	Severity	WDPT (s)	Infil (ml/min)
125	H3-1-0m-0	H	182	4.0
126	H3-1-0m-120	H	16	8.0
127	H3-1-0m-240	H	9	17.0
128	H3-1-50m-0	H	0	12.0
129	H3-1-50m-240-1	H	27	2.3
130	H3-1-50m-240-2	H	198	3.8
131	H3-1-200m-0	H	226	1.3
132	H3-1-200m-120	H	107	4.8
133	H3-1-200m-240	H	36	7.0
134	H3-2-0m-0	H	6	11.0
135	H3-2-0m-120	H	14	9.0
136	H3-2-0m-240	H	96	2.7
137	H3-2-50m-0	H	183	0.0
138	H3-2-50m-120	H	202	0.7
139	H3-2-50m-240	H	103	5.5
140	H3-2-200m-0	H	251	3.7
141	H3-2-200m-120	H	124	0.3
142	H3-2-200m-240	H	22	10.0
143	H4-1-0m0	H	57	3.0
144	H4-1-0m120	H	231	2.3
145	H4-1-0m240	H	139	2.0
146	H4-1-50M-0	H	220	1.8
147	H4-1-50m-120	H	111	3.9
148	H4-1-50m240	H	180	0.8
149	H4-1-200m0	H	300	0.3
150	H4-1-200m120	H	16	8.5
151	H4-1-200m240	H	41	4.9
152	H4-2-0m-0	H	138	5.3
153	H4-2-0m-120	H	51	5.5
154	H4-2-0m-240	H	174	4.0
155	H4-2-50m-0	H	164	4.0
156	H4-2-50m-120	H	250	0.0
157	H4-2-50m-240	H	237	1.0
158	H4-2-200m-0	H	176	3.8
159	H4-2-200m-120	H	74	0.3
160	H4-2-200m-240	H	115	3.5
161	H5-1-0m-0	H	84	4.5
162	H5-1-0m-120	H	209	1.0
163	H5-1-0m-240	H	47	15.0
164	H5-1-50m-0	H	239	6.8
165	H5-1-50m-120	H	10	7.0
166	H5-1-50m-240	H	8	4.3
167	H5-1-200m-0	H	18	5.3
168	H5-1-200m-120	H	129	5.0
169	H5-1-200m-240	H	40	5.3
170	H5-1-250m-0	H	149	1.8
171	H5-1-250m-120	H	151	4.0
172	H5-1-250m-240	H	26	2.3
173	H5-1-400m-0	H	32	4.8
174	H5-1-400m-120	H	53	8.3
175	H5-1-400m-240	H	136	0.0
176	H5-2-0m-0	H	12	9.0
177	H5-2-0m-120	H	21	7.8
178	H5-2-0m-240	H	43	6.8
179	H5-2-50m-0	H	138	0.0
180	H5-2-50m-120	H	101	1.5
181	H5-2-50m-240	H	126	2.8
182	H5-2-200m-0	H	16	10.8
183	H5-2-200m-120	H	204	1.8
184	H5-2-200m-240	H	144	0.0

Figure Appendix B3. High burn severity WDPT and Infiltrometer values.

APPENDIX C  
BURN SEVERITY DATA

Number	Easting (m)	Northing (m)	OM (%)	soil (%)	ash (%)	litter (%)	litter (mm)	new lit. (%)	new lit. (mm)	humus (%)	humus (mm)
1	473806	4318852	4.7	28	57	9	2	0	0	0	0
2	473830	4318823	6.4	0	7	90	20	35	2	0	0
3	473796	4318823	6.7	0	16	43	0	5	0	38	0
4	473862	4318851	4.2	81	0	15	3	25	1	0	0
5	473879	4318821	7.8	6	0	86	0	65	0	0	0
6	473845	4318821	3.7	7	0	90	12	25	2	0	0
7	474011	4318876	4.4	1	14	79	0	2	0	0	0
8	474028	4318846	4.2	2	5	91	0	1	0	0	0
9	473994	4318846	4.9	25	5	64	0	1	0	0	0
10	473814	4318920	2.3	2	3	91	10	95	2	0	0
11	473831	4318890	1.1	5	10	62	10	10	3	0	0
12	473797	4318890	1.2	98	0	0	2	1	1	0	0
13	473958	4318919	11.2	20	10	64	10	3	1	0	0
14	473975	4318889	1.9	0	53	42	5	2	1	0	0
15	473941	4318889	3.3	5	15	77	15	3	1	0	0
16	474007	4318925	2.1	2	86	9	5	2	1	0	0
17	474024	4318895	11.1	34	15	49	10	1	1	0	0
18	473990	4318895	7.7	15	1	82	10	1	1	0	0
19	482014	4333206	2.8	6	6	63	15	85	4	0	0
20	482031	4333176	1.7	4	4	83	10	65	6	0	0
21	481997	4333176	3.1	11	64	21	7	50	8	0	0
22	482065	4333205	2.8	47	0	47	10	0	0	0	0
23	482082	4333175	3.7	6	6	59	10	80	4	0	0
24	482048	4333175	4.3	1	13	81	8	20	2	0	0
25	482215	4333214	3.4	1	1	97	9	2	4	0	0
26	482232	4333184	1.3	10	5	81	5	2	0	0	0
27	482198	4333184	1.3	5	14	75	4	2	1	0	0
28	482114	4333249	2.9	48	16	32	7	1	2	0	0
29	482131	4333219	3.6	19	38	38	2	15	2	0	0
30	482097	4333219	1.6	1	31	36	12	5	2	0	0
31	482165	4333256	5.6	76	6	14	8	1	2	0	0
32	482182	4333226	2.2	10	1	82	7	5	2	0	0
33	482148	4333226	2.5	1	1	81	15	4	2	0	0
34	466322	4327069	6.3	78	8	8	2	1	0	0	0
35	466339	4327039	3.7	58	10	29	8	10	1	0	0
36	466305	4327039		81	6	6	0	1	0	0	0
37	466369	4327051	7.3	49	36	13	1	1	0	0	0
38	466386	4327021	4.1	20	20	59	20	50	1	0	0
39	466352	4327021	5.2	67	10	19	2	2	1	0	0
40	466511	4327002	4.5	48	29	19	2	2	0	0	0
41	466528	4326972		39	29	29	1	35	1	0	0
42	466494	4326972	2.1	91	5	0	0	1	0	0	0
43	466557	4326980	6.2	56	28	9	0	20	2	0	0
44	466574	4326950	2.5	85	0	9	2	1	0	0	0
45	466540	4326950		49	39	10	2	1	0	0	0
46	466710	4326927	4.13	39	10	49	15	5	1	0	0
47	466727	4326897	18.4	32	18	37	3	15	1	0	0
48	466693	4326897	9.0	54	5	36	10	2	1	0	0
49	467547	4324362	20.5	28	14	52	2	1	1	0	0
50	467564	4324332	20.4	5	11	74	5	10	2	0	0
51	467530	4324332	6.4	48	24	24	2	20	1	0	0
52	467597	4324362	4.4	68	10	10	2	1	0	0	0
53	467614	4324332	8.4	61	0	24	3	3	1	0	0
54	467580	4324332		9	9	45	10	80	2	0	0
55	467691	4324450	6.8	6	71	18	5	10	1	0	0
56	467708	4324420	1.1	2	19	77	10	1	1	0	0
57	467674	4324420	3.3	2	0	85	15	60	2	0	0
58	467576	4324459	8.2	3	87	7	2	3	1	0	0
59	467593	4324429	4.8	86	6	6	5	1	1	0	0
60	467559	4324429	10.8	1	25	70	6	1	1	0	0
61	467689	4324478	18.6	49	22	27	10	0	0	0	0
62	467706	4324448	16.3	1	0	97	12	0	0	0	0
63	467672	4324448	12.2	1	0	96	15	1	1	0	0

Figure Appendix C1. Low burn severity subplot data. Easting and Northing are UTM coordinates in meters. OM is calculated by mass from surface soil samples. Ground cover components with (%) are percent cover and cover components with (mm) are average depth.

Number	BCC (%)	CWD <3" (%)	CWD >3" (%)	Aspect (degree)	Slope (%)	Trees (#)	Slope Position	Rock (%)	Stumps (%)	Water (%)
1	0	4	0	90	5	9	low	0	2	0
2	0	3	0	5	10	7	low	0	0	0
3	0	1	2	90	5	7	low	0	0	0
4	0	1	3	3	5	12		0	0	0
5	6	3	0	10	10	9		0	0	0
6	0	0	3	0	5	8		0	0	0
7	0	3	4	340	25	12	low	0	0	0
8	0	2	0	0	12	9	mid	0	0	0
9	0	2	0	20		11	mid	0	5	0
10	0	1	2	90	20	8	mid	1	0	0
11	0	10	14	0	15	7	low	0	0	0
12	0	1	1	45	25	4	mid	0	0	0
13	0	5	0	45	12	6	high	2	0	0
14	0	2	3	45	10	7	high	0	0	0
15	0	2	0	90	7	4	high	0	0	0
16	0	1	2	23	11	11	mid	0	0	0
17	0	1	1	90	15	7	mid	0	0	0
18	0	1	1	90	15	5	mid	0	0	0
19	6	19	0	340	15	6	mid	0	0	0
20	4	4	0	33	15	5	top	0	0	0
21	2	2	0	324	15	3	top	0	0	0
22	1	5	0	325	15	1	top	0	0	0
23	6	18	6	330	15	3	top	0	0	0
24	1	1	3	350	15	5	top	0	0	0
25	0	1	0	270	10	5	top	0	0	0
26	0	5	0	320	9	9		0	0	0
27	0	5	2	330	12	7		0	0	0
28	2	2	0	210	15	2	low	0	0	0
29	0	4	1	320	10	7		0	1	0
30	15	15	1	330	15	6	low	0	0	0
31	1	1	0	240	10	2	top	0	1	0
32	1	5	0	250	10	4		0	0	0
33	1	16	0	320	5	7	top	0	0	0
34	0	3	2	230	8	1	low	2	0	0
35	0	2	0	220	6	4	low	1	0	0
36	0	1	0	220	11	0	low	6	0	0
37	0	2	0	130	5	3	low	0	0	0
38	0	1	1	140	5	5	low	0	0	0
39	0	1	1	200	7	3	low	2	0	0
40	0	1	1	250	15	1	low	0	2	0
41	0	1	0	260	18	6	mid	2	0	0
42	0	2	1	250	9	0	low	1	0	0
43	0	2	0	230	10	5	top	4	1	0
44	0	1	0	200	13	0	mid	5	0	0
45	0	1	1	240	12	10	mid	0	0	0
46	0	3	0	250	12	6	mid	0	0	0
47	0	5	3	210	12	9	mid	5	1	0
48	0	3	1	250	12	8	mid	1	1	0
49	0	1	0	0	26	7	mid	5	0	0
50	0	5	2	0	26	3	mid	2	0	0
51	0	1	2	0	26	6	mid	1	0	0
52	0	2	5	300	33	12	mid	5	1	0
53	0	6	0	300	26	2	mid	9	0	0
54	0	18	9	340	36	5	mid	9	0	0
55	1	4	0	0	25	6	mid	1	0	0
56	0	2	0	0	25	5	mid	0	0	0
57	0	4	9	330	25	4	mid	0	0	0
58	0	3	0	330	30	6	mid	0	0	0
59	0	1	0	290	22	5		0	0	0
60	0	2	1	290	25	6		1	0	0
61	0	1	0	280	35	2	mid	1	0	0
62	0	2	0	260	22	20	mid	0	0	0
63	0	2	0	10	33	12	mid	1	0	0

Figure Appendix C2. Low burn severity subplot data continued. Numbering system remains consistent throughout data sheets. Ground cover components with (%) are percent cover and cover components with (#) are counts per subplot.

Number	Easting (m)	Northing (m)	OM (%)	soil (%)	ash (%)	litter (%)	litter (mm)	new lit. (%)	new lit. (mm)	humus (%)	humus (mm)
64	473980	439351	0.1	54	43	0	4	30	2	0	0
65	473997	439321	2.4	74	5	20	3	25	2	0	0
66	473963	439321	2.6	69	16	12	2	3	1	0	0
67	474030	439351	5.1	24	24	49	5	60	2	0	0
68	474047	439321	4.6	69	20	10	5	1	1	0	0
69	474013	439321	2.8	28	19	47	5	30	2	0	0
70	474177	439338	2.6	10	10	77	10	50	2	0	0
71	474160	439308	2.0	40	20	30	7	1	1	0	0
72	474160	439308	4.1	63	21	16	5	5	2	0	0
73	474024	4342236	3.0	65	5	28	2	1	0	0	0
74	474041	4342206	4.2	29	10	59	2	10	1	0	0
75	474007	4342206		82	5	10	2	2	0	0	0
76	474073	4342236	2.5	82	5	10	3	0	0	0	0
77	474090	4342206	2.7	6	38	51	6	20	7	0	0
78	474056	4342206	2.8	26	35	35	2	40	6	0	0
79	474221	4342218	1.5	88	5	5	1	3	0	0	0
80	474238	4342188	2.2	74	5	5	1	1	1	0	0
81	474204	4342188	2.1	85	6	6	1	1	0	0	0
82	473770	4342420	5.2	74	12	12	8	20	3	0	0
83	473787	4342390	2.1	88	5	5	4	1	4	0	0
84	473753	4342390	2.7	26	32	39	8	20	2	0	0
85	473821	4342422	5.0	47	23	23	6	60	10	0	0
86	473838	4342392	7.0	62	15	15	4	30	7	0	0
87	473804	4342392		87	5	5	6	1	1	0	0
88	473965	4342424	3.3	94	0	5	8	0	0	0	0
89	473982	4342394	4.1	29	29	29	6	75	7	0	0
90	473948	4342394	4.2	20	10	69	5	60	3	0	0
91	481620	4333315	12	47	28	19	1	10	2	0	0
92	481620	4333315	2.5	37	9	46	3	30	2	0	0
93	481586	4333315		20	5	71	15	1	0	0	0
94	481652	4333352	2.6	49	10	39	3	5	0	0	0
95	481669	4333322	2.1	5	5	88	3	90	3	0	0
96	481635	4333322	5.3	18	14	45	5	5	1	0	0
97	481802	4333351	2.5	20	20	59	3	30	2	0	0
98	481819	4333321	12	28	47	19	2	1	0	0	0
99	481785	4333321	2.9	64	9	18	2	20	1	0	0
100	481701	4333299	2.4	10	10	78	5	80	10	0	0
101	481718	4333269	4.9	39	29	29	3	30	3	0	0
102	481684	4333269	3.0	45	9	36	2	30	3	0	0
103	481751	4333300	13	34	5	58	1	60	1	0	0
104	481768	4333270	2.6	29	20	49	2	15	1	0	0
105	481734	4333270	3.3	20	10	69	2	60	3	0	0
107	476218	4325456	11.4	19	19	57	2	2	0	0	0
108	476235	4325426	6.3	40	5	40	3	3	1	10	5
109	476201	4325426	8.2	9	3	38	5	5	1	50	20
110	476268	4325456		9	5	80	20	2	1	0	0
111	476285	4325426	9.0	10	1	86	10	1	0	0	0
112	476251	4325426	3.5	35	7	21	2	20	1	14	5
113	476419	4325450	9.9	5	5	87	15	1	0	0	0
114	476436	4325420	3.7	16	4	53	5	5	1	20	10
115	476402	4325420	4.4	47	19	28	3	10	1	0	0
116	476267	4325391	3.5	10	1	88	10	1	1	0	0
117	476284	4325361	4.0	5	78	14	3	1	1	0	0
118	476250	4325361	1.9	68	15	15	5	1	1	0	0
119	476413	4325396	3.7	5	10	84	20	1	1	0	0
120	476430	4325366	4.9	5	29	63	3	1	1	0	0
121	476396	4325366	2.5	13	1	82	10	1	1	0	0
122	476463	4325396	1.5	69	5	20	0	30	0	0	0
123	476480	4325366	1.4	10	20	69	6	2	0	0	0
124	476446	4325366	9.1	20	10	66	12	2	1	0	0

Figure Appendix C3. Moderate burn severity subplot data. Easting and Northing are UTM coordinates in meters. OM is calculated by mass from surface soil samples. Ground cover components with (%) are percent cover and cover components with (mm) are average depth.

Number	BCC (%)	CWD <3" (%)	CWD >3" (%)	Aspect (degree)	Slope (%)	Trees (#)	Slope Position	Rock (%)	Stumps (%)	Water (%)
64	0	2	0	90	35	3	low	0	0	0
65	0	0	0	85	22	1	mid	1	0	0
66	0	2	1	290	22	6	low	0	0	0
67	0	2	0	310	25	7	low	0	0	0
68	0	1	0	315	20	5	top	0	0	0
69	0	4	1	300	22	4	mid	1	0	0
70	2	2	0	18	15	8	low	0	0	0
71	0	1	0	25	15	4	low	10	0	0
72	0	1	0	40	15	2	low	0	0	0
73	0	2	0	360	6	2	low	0	0	0
74	0	2	0	20	18	9	low	0	0	0
75	1	1	0	20	20	8	mid	0	0	0
76	1	1	0	225	5	4	low	1	0	0
77	1	1	0	330	10	6	mid	0	1	0
78	0	2	0	15	15	8	mid	0	2	0
79	0	0	0	328	0	7	top	0	2	0
80	0	1	0	270	20	4	top	15	1	0
81	1	1	0	230	15	2	mid	0	0	0
82	1	0	0	350	15	3	mid	0	0	0
83	1	1	0	340	15	4		0	0	0
84	1	1	0	312	5	3	mid	0	0	0
85	0	2	0	25	10	2	mid	0	5	0
86	0	8	0	30	15	2	mid	0	0	0
87	1	1	0	30	15	2	mid	0	1	0
88	0	1	0	40	20	4	low	0	0	0
89	0	6	0	352	20	9	low	6	0	0
90	0	1	0	10	29	10	high	0	0	0
91	0	1	5	230	8	2	mid	1	0	0
92	0	2	2	260	12	5	low	5	0	0
93	0	3	0	210	9	4	mid	0	0	0
94	0	2	0	210	10	2	mid	0	0	0
95	0	2	0	280	7	10	mid	0	0	0
96	0	3	2	230	7	2	low	18	0	0
97	0	1	1	90	2	4	top	0	0	0
98	0	2	5	80	22	12	mid	0	0	0
99	0	3	1	200	7	5	high	0	5	0
100	0	1	2	190	4	3	mid	0	0	0
101	0	2	0	160	12	3	mid	0	0	0
102	0	9	0	290	24	2	low	0	0	0
103	0	2	0	340	12	3	mid	1	0	0
104	0	1	1	230	6	5	high	0	0	0
105	0	1	0	210	12	11	mid	0	0	0
107	0	1	3	360	17	9	mid	0	1	0
108	0	3	2	350	19	13	high	0	0	0
109	0	0	0	350	26	7	high	0	1	0
110	0	5	1	350	25	9	mid	0	0	0
111	0	2	1	320	8	9	top	1	0	0
112	4	4	4	338	23	14	high	0	12	0
113	0	2	0	110	7	7	top	1	1	0
114	2	2	1	146	5	9	high	0	0	0
115	0	1	5	130	11	9	mid	0	0	0
116	0	1	0	9	18	9	top	0	0	0
117	0	2	2	20	24	5	high	0	0	0
118	0	1	1	200	27	8	high	1	0	0
119	0	1	0	104	25	4	high	0	0	0
120	0	1	1	60	18	8		0	1	0
121	0	5	0	200	17	10	high	0	0	0
122	0	2	3	170	9	10	mid	0	1	0
123	0	2	0	220	5	10	low	0	0	0
124	0	2	1	170	10	7	low	0	1	0

Figure Appendix C4. Moderate burn severity subplot data continued. Numbering system remains consistent throughout data sheets. Ground cover components with (%) are percent cover and cover components with (#) are counts per subplot.

Number	Easting (m)	Northing (m)	OM (%)	soil (%)	ash (%)	litter (%)	litter (mm)	new lit. (%)	new lit. (mm)	humus (%)	humus (mm)
125	468992	4335341	4.25	72	20	5	1	0	1	0	0
126	469009	4335311	2.23	80	5	9	1	0	1	0	0
127	468975	4335311	3.03	69	24	5	1	1	1	0	0
128	469042	4335341	4.33	92	5	1	0	0	0	0	0
129	469025	4335311	2.42	84	8	2	0	0	0	0	0
130	469025	4335311	2.33	47	30	2	0	0	0	0	0
131	469187	4335341	2.60	57	35	5	0	1	0	0	0
132	469204	4335311	1.95	89	3	2	1	5	1	0	0
133	469170	4335311	2.03	90	5	1	1	1	1	0	0
134	468986	4335289	2.06	55	25	15	0	0	0	0	0
135	469003	4335259	3.70	84	10	5	1	0	0	0	0
136	468969	4335259	3.14	72	20	0	0	1	0	0	0
137	469036	4335289	7.20	55	40	2	1	1	1	0	1
138	469053	4335259	5.45	23	51	10	1	1	0	0	0
139	469019	4335259	5.20	59	20	10	0	0	0	0	0
140	469185	4335291	6.37	68	21	5	1	5	1	1	0
141	469202	4335261	7.61	51	34	11	1	10	1	1	0
142	469168	4335261	1.92	94	2	1	0	1	0	0	0
143	475783	4328505	5.33	19	76	0	0	0	0	0	0
144	475800	4328475	3.91	4	73	17	2	0	0	0	0
145	475766	4328475	3.49	38	38	19	0	0	0	0	0
146	475833	4328505	1.35	29	67	2	1	0	0	0	0
147	475850	4328475		58	19	19	1	0	0	0	0
148	475816	4328475	27.33	5	64	28	2	0	0	0	0
149	475981	4328512	4.81	69	29	0	0	0	0	0	0
150	475998	4328482	1.42	71	9	14	1	0	0	2	2
151	475964	4328482	4.74	28	42	23	2	0	0	0	0
152	475779	4328541	0.32	49	20	29	8	0	0	0	0
153	475796	4328511	11.64	20	49	29	6	0	0	0	0
154	475762	4328511	10.58	5	78	15	7	0	0	0	0
155	475831	4328544	6.00	85	5	10	3	0	0	0	0
156	475848	4328514	4.81	39	39	19	9	0	0	0	0
157	475814	4328514	4.84	10	29	39	12	0	0	0	0
158	475979	4328560	7.00	13	44	38	9	0	0	0	0
159	475996	4328530	2.90	27	55	9	1	0	0	0	0
160	475962	4328530	8.23	59	10	29	10	0	0	0	0
161	468421	4332331	4.63	91	0	2	1	2	1	0	0
162	468438	4332301	10.60	69	15	15	1	1	1	0	0
163	468404	4332301	5.86	87	0	5	0	5	0	0	0
164	468471	4332331	4.14	17	80	0	0	1	0	0	0
165	468488	4332301	6.39	94	0	5	1	1	1	0	0
166	468454	4332301	3.24	79	5	15	1	1	1	0	0
167	468621	4332331	2.49	67	10	21	0	1	0	0	0
168	468638	4332301	3.58	65	15	15	3	5	0	0	0
169	468604	4332301	5.54	51	0	30	1	2	1	17	2
170	468668	4332330	4.46	42	16	42	0	1	1	0	0
171	468685	4332300	2.40	44	11	44	1	15	1	0	0
172	468651	4332300	7.02	83	0	16	1	5	1	0	0
173	468819	4332333	2.74	44	5	49	3	20	2	0	0
174	468835	4332303	5.55	57	6	34	3	1	1	0	0
175	468801	4332303	3.12	82	10	5	1	3	1	0	0
176	468413	4332278	6.18	44	20	34	2	1	1	0	0
177	468430	4332248	5.25	78	5	16	1	1	1	0	0
178	468396	4332248	2.37	81	1	16	1	1	1	0	0
179	468463	4332278	4.59	75	19	3	1	1	1	0	0
180	468480	4332248	1.72	83	10	5	1	1	1	0	0
181	468446	4332248	6.92	92	5	1	1	1	1	0	0
182	468612	4332278	2.35	92	0	5	1	1	1	1	1
183	468629	4332248	3.18	78	10	10	1	1	0	0	0
184	468595	4332248	6.94	57	19	19	1	1	0	0	0

Figure Appendix C5. High burn severity subplot data. Easting and Northing are UTM coordinates in meters. OM is calculated by mass from surface soil samples. Ground cover components with (%) are percent cover and cover components with (mm) are average depth.

Number	BCC (%)	CWD <3" (%)	CWD >3" (%)	Aspect (degree)	Slope (%)	Trees (#)	Slope Position	Rock (%)	Stumps (%)	Water (%)
125	0	0	1	112	10	7	upper	1	1	0
126	0	1	0	162	30	1	upper	5	0	0
127	0	1	0	112	30	0	upper	1	0	0
128	0	1	0	70	35	2	upper	1	0	0
129	0	1	3	130	30	3	mid	1	0	0
130	0	1	5	158	30	2	upper	15	0	0
131	0	1	0	212	30	6	top	2	0	0
132	0	2	1	202	30	7	high	3	0	0
133	0	1	0	188	35	1	bottom	3	0	0
134	0	2	0	100	30	1	mid	3	0	0
135	0	1	0	122	25	5	top	0	0	0
136	5	1	0	162	30	9	mid	2	0	0
137	0	1	1	357	38	3	mid	1	0	0
138	5	5	5	120	25	2	toe	1	0	0
139	0	1	10	83	30	4	shoulder	0	0	0
140	0	2	1	238	47	5	mid	1	0	0
141	0	2	0	212	40	5	mid	0	0	0
142	0	1	0	183	35	2	low	1	0	0
143	0	1	3	70	8	13	low	1	0	0
144	0	2	1	66	12	9	toe	0	3	0
145	0	3	1	50	12	12	low	0	0	0
146	0	1	1	60	9	7	bottom	0	0	0
147	0	1	0	360	30	1	low	3	0	0
148	2	1	1	86	14	10	bottom	0	0	0
149	0	1	1	70	14	14	bottom	0	0	0
150	0	1	1	46	20	6	shoulder	2	0	0
151	0	3	5	44	10	2	bottom	0	0	0
152	0	1	1	270	5	3	low	0	0	0
153	1	1	0	20	5	8	low	0	0	0
154	1	1	1	170	20	8	low	0	0	0
155	0	0	0	180	20	1	high	0	0	0
156	1	1	1	75	2	6	bottom	0	0	0
157	20	1	1	60	5	5	low	0	0	0
158	0	6	0	38	10	7	mid	0	0	0
159	1	3	5	95	8	5	low	0	1	0
160	0	1	0	90	27	5	mid	1	0	0
161	0	1	0	47	3	4	top	0	5	0
162	0	1	0	96	6	2	top	0	0	0
163	1	1	5	108	7	1	top	0	0	0
164	0	1	0	42	6	5	top	1	0	0
165	0	0	0	120	9	0	top	1	0	0
166	0	1	0	88	7	2	top	0	0	0
167	1	1	0	27	8	8	top	0	0	0
168	0	2	1	18	5	5	top	0	0	0
169	0	2	0	20	3	2	top	0	0	0
170	0	1	0	5	7	9	top	0	0	0
171	0	0	0	350	2	8	top	0	0	0
172	0	1	0	354	2	3	top	0	0	0
173	0	1	0	345	13	4	top	0	0	0
174	1	1	0	184	0	0	top	1	0	0
175	0	1	1	353	2	1	top	0	0	0
176	0	1	1	86	6	4	top	0	0	0
177	0	1	0	123	8	0	top	0	0	0
178	0	1	0	128	9	3	top	1	0	0
179	0	3	0	76	6	3	top	0	0	0
180	0	1	1	110	6	1	top	0	0	0
181	0	1	0	6	66	6	top	0	1	0
182	0	1	0	10	7	6	top	0	1	0
183	0	1	0	210	10	4	mid	1	0	0
184	0	1	2	180	14	5	top	2	0	0

Figure Appendix C6. High burn severity subplot data continued. Numbering system remains consistent throughout data sheets. Ground cover components with (%) are percent cover and cover components with (#) are counts per subplot.

APPENDIX D  
EXAMPLES FROM SAS:  
STATISTICAL CODES AND OUTPUT

```

data;
input class $ WD infil;
cards;
L      214    1.33
L      111    1.75
L      86     2.33
.
.
.
M      21     4.5
M      274    0.2
M      99     0.9
.
.
.
H      16     10.8
H      204    1.8
H      144    0.0
;
proc npar1way wilcoxon;
class class;
var WD;
run;

```

Figure Appendix D1. Sample SAS code for NPAR1WAY; a one-way statistical test for non-normally distributed data, testing the significance of WDPT and Infiltration values at the three burn severity levels, low (L), moderate (M), and high (H).

The SAS System  
The NPAR1WAY Procedure  
Wilcoxon Scores (Rank Sums) for Variable WDPT  
Classified by Variable SITE

Mean			Sum of	Expected	Std Dev
Score	SITE	N	Scores	Under H0	Under H0
82.523810	L	63	5199.0	5764.50	338.109932
110.423729	M	59	6515.0	5398.50	332.653988
82.316667	H	60	4939.0	5490.00	334.094798

Average scores were used for ties.

Kruskal-Wallis Test

Chi-Square	11.2655
DF	2
Pr > Chi-Square	0.0036

The NPAR1WAY Procedure  
Wilcoxon Scores (Rank Sums) for Variable INFIL  
Classified by Variable SITE

Mean			Sum of	Expected	Std Dev
Score	SITE	N	Scores	Under H0	Under H0
101.174603	L	63	6374.00	5764.50	337.996832
78.754237	M	59	4646.50	5398.50	332.542713
93.875000	H	60	5632.50	5490.00	333.983041

Average scores were used for ties.

Kruskal-Wallis Test

Chi-Square	5.7042
DF	2
Pr > Chi-Square	0.0577

Figure Appendix D2. SAS output from non-parametric statistical test NPAR1WAY.

```
data;
    input WDPT Infil OM;
cards;
298 0.00 41.3
180 0.8 27.33
185 9.00 20.5
.
.
.
.
.
;
proc corr spearman;
var WDPT Infil;
run;
proc corr spearman;
var WDPT OM;
run;
```

Figure Appendix D3. SAS code for Spearman correlation for non-normally distributed data.

The SAS System  
The CORR Procedure

2 Variables: WDPT Infil

Simple Statistics

Variable	N	Mean	Std Dev	Median	Minimum	Maximum
WDPT	173	125.97110	90.87408	123.00000	0	300.00000
Infil	173	4.39364	3.42007	3.80000	0	17.00000

Spearman Correlation Coefficients, N = 173  
Prob > |r| under H0: Rho=0

	WDPT	Infil
WDPT	1.00000	-0.65422 <.0001
Infil	-0.65422 <.0001	1.00000

The SAS System  
The CORR Procedure

2 Variables: WDPT OM

Simple Statistics

Variable	N	Mean	Std Dev	Median	Minimum	Maximum
WDPT	173	125.97110	90.87408	123.00000	0	300.00000
OM	173	5.11549	4.77900	3.91000	0.10000	41.30000

Spearman Correlation Coefficients, N = 173  
Prob > |r| under H0: Rho=0

	WDPT	OM
WDPT	1.00000	0.14170 0.0629
OM	0.14170 0.0629	1.00000

Figure Appendix D4. Sample SAS Spearman correlation output for WDPT with Infiltrator and OM values.

APPENDIX E  
SAMPLE EIGENVECTOR AND  
COVARIANCE STATISTICS FOR  
PRINCIPAL COMPONENT BANDS 1–10

	1	2	3	4	5	6	7	8	9	10	Total Variance
Eigenvalues	62296253	1692835.2	37742.7	19228.9	8603.8	6168.3	4253.2	3490.9	1919.5	903.3	64071399.1
Difference	60603418	1655092.5	18513.7	10625.1	2435.5	1915.2	762.3	1571.4	1016.2	-	
Variance by PC	97.229	2.642	0.059	0.030	0.013	0.010	0.007	0.005	0.003	0.001	100
		99.872	99.930	99.960	99.974	99.984	99.990	99.996	99.999	100.000	
Covariance Matrix											
	Band 71	Band 72	Band 73	Band 74	Band 75	Band 76	Band 77	Band 78	Band 79	Band 80	
71	1234497										
72		1220891									
73			1244928								
74				1251594							
75					1279905						
76						1302619					
77							1352264				
78								1392507			
79									1436924		
80										1476893	
Eigenvectors	1	2	3	4	5	6	7	8	9	10	
71	0.140	0.072	-0.269	-0.458	0.096	0.105	0.092	0.328	-0.504	-0.042	
72	0.139	0.079	-0.307	-0.248	0.056	-0.029	0.039	0.201	0.039	-0.009	
73	0.140	0.092	-0.243	-0.196	0.009	-0.080	0.062	0.094	0.195	0.006	
74	0.141	0.103	-0.168	-0.173	-0.024	-0.098	0.085	0.005	0.261	0.043	
75	0.142	0.113	-0.103	-0.156	-0.054	-0.098	0.101	-0.054	0.261	0.102	
76	0.143	0.121	-0.072	-0.109	-0.066	-0.158	0.107	-0.010	0.163	-0.013	
77	0.146	0.130	-0.021	-0.088	-0.066	-0.128	0.108	-0.053	0.107	0.071	
78	0.148	0.138	0.015	-0.065	-0.073	-0.178	0.118	-0.021	0.018	-0.077	
79	0.150	0.146	0.015	0.004	-0.030	-0.115	0.098	-0.078	-0.001	0.145	
80	0.152	0.155	0.042	0.028	-0.009	-0.134	0.119	-0.078	-0.064	0.050	
Correlation	1	2	3	4	5	6	7	8	9	10	
71	0.993	0.085	-0.047	-0.057	0.008	0.007	0.005	0.017	-0.020	-0.001	
72	0.994	0.093	-0.054	-0.031	0.005	-0.002	0.002	0.011	0.002	0.000	
73	0.993	0.107	-0.042	-0.024	0.001	-0.006	0.004	0.005	0.008	0.000	
74	0.992	0.119	-0.029	-0.022	-0.002	-0.007	0.005	0.000	0.010	0.001	
75	0.991	0.130	-0.018	-0.019	-0.004	-0.007	0.006	-0.003	0.010	0.003	
76	0.990	0.138	-0.012	-0.013	-0.005	-0.011	0.006	-0.001	0.006	0.000	
77	0.989	0.145	-0.004	-0.010	-0.005	-0.009	0.006	-0.003	0.004	0.002	
78	0.988	0.152	0.002	-0.008	-0.006	-0.012	0.007	-0.001	0.001	-0.002	
79	0.987	0.158	0.003	0.000	-0.002	-0.008	0.005	-0.004	0.000	0.004	
80	0.986	0.166	0.007	0.003	-0.001	-0.009	0.006	-0.004	-0.002	0.001	

Figure Appendix E1. Flight line 4 eigenvectors and correlation values between wavebands 71-80 and PC bands 1-10.

PC Bands	1	2	3	4	5	6	7	8	9	10	Total
Eigenvalue	2.6E+07	518642	10476.1	6371.16	3746.64	2633.23	1178.1	963.491	850.964	598.609	2.6E+07
Difference	2.5E+07	508166	4104.97	2624.52	1113.41	1455.13	214.605	12.527	252.355	-	
Variance %	97.924	1.974	0.040	0.024	0.014	0.010	0.004	0.004	0.003	0.002	100.00
<b>Covariance Matrix</b>											
	Band 71	Band 72	Band 73	Band 74	Band 75	Band 76	Band 77				
71	434431										
72		439389									
73			422485								
74				41124							
75					408037						
76						403676					
77							405102				
<b>Eigenvectors</b>											
	1	2	3	4	5	6	7	8	9	10	
71	0.129	0.114	-0.077	-0.549	-0.077	0.100	-0.082	0.229	-0.231	0.400	
72	0.129	0.116	-0.177	-0.378	-0.108	-0.021	0.040	0.134	-0.067	-0.119	
73	0.127	0.123	-0.164	-0.272	-0.072	-0.061	0.091	0.029	-0.018	-0.160	
74	0.125	0.131	-0.127	-0.213	-0.029	-0.073	0.105	-0.042	-0.001	-0.182	
75	0.124	0.135	-0.138	-0.135	0.031	-0.038	0.196	-0.088	0.034	-0.063	
76	0.124	0.144	-0.060	-0.121	-0.008	-0.150	0.049	-0.073	-0.043	-0.129	
77	0.124	0.149	-0.032	-0.074	0.015	-0.101	0.047	-0.085	-0.029	-0.039	
<b>Correlation</b>											
	1	2	3	4	5	6	7	8	9	10	
71	0.990	0.124	-0.012	-0.066	-0.007	0.008	-0.004	0.011	-0.010	0.015	
72	0.991	0.126	-0.027	-0.046	-0.010	-0.002	0.002	0.006	-0.003	-0.004	
73	0.990	0.136	-0.026	-0.033	-0.007	-0.005	0.005	0.001	-0.001	-0.006	
74	0.989	0.147	-0.020	-0.026	-0.003	-0.006	0.006	-0.002	0.000	-0.007	
75	0.988	0.152	-0.022	-0.017	0.003	-0.003	0.011	-0.004	0.002	-0.002	
76	0.986	0.163	-0.010	-0.015	-0.001	-0.012	0.003	-0.004	-0.002	-0.005	
77	0.986	0.168	-0.005	-0.009	0.001	-0.008	0.003	-0.004	-0.001	-0.001	

Figure Appendix E2. Flight line 7 eigenvectors and correlation values between wavebands 71-77 and PC bands 1-10.

APPENDIX F

PICTURES

HAYMAN FIRE  
Pike-San Isabel National Forests  
June 2002

### BAER Burn Severity

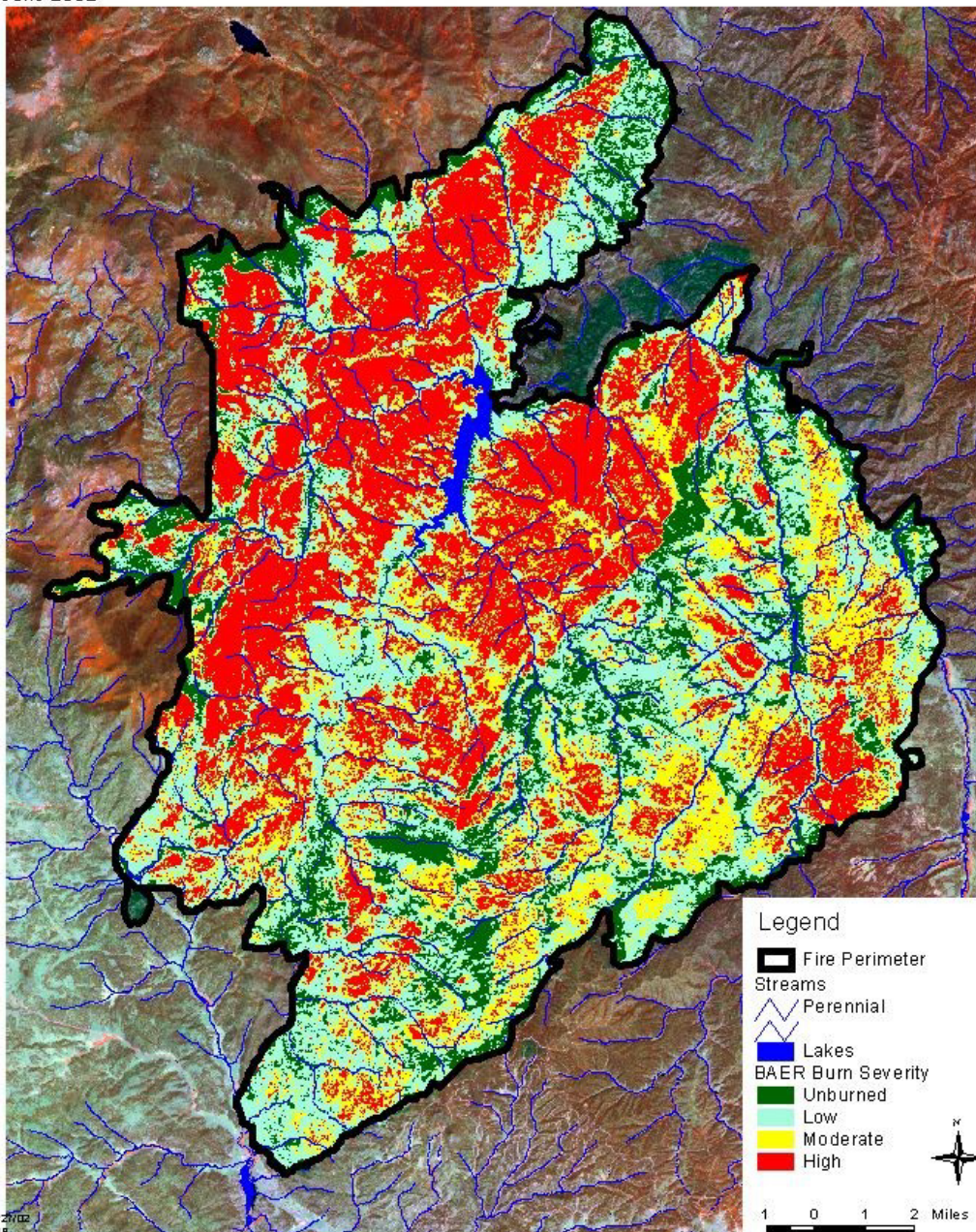


Figure Appendix F1. BAER burn severity map.



Figure Appendix F2. Mini-disk infiltrometer test (top) and water drop penetration time test (bottom). Both were taken at the same high burn severity site on the Hayman Fire on July 30<sup>th</sup>, 2002. Surface ash was removed to reveal the mineral soil for the tests.